④

NSWC TR 88-146

AD-A211 936

GRAPHITE HEATING ELEMENT THERMAL AND STRUCTURAL PERFORMANCE IN THE NSWC HYPERVELOCITY WIND TUNNEL 9 - A FINITE ELEMENT ANALYSIS

BY   MICHAEL A. METZGER

STRATEGIC SYSTEMS DEPARTMENT

JUNE 1988

DTIC
ELECTE
SEP 0 5 1989
S D
D

NAVAL SURFACE WARFARE CENTER

Dahlgren, Virginia 22448-5000 ● Silver Spring, Maryland 20903-5000

89   9 01139

REPORT DOCUMENTATION PAGE

1a. REPORT SECURITY CLASSIFICATION UNCLASSIFIED		1b RESTRICTIVE MARKINGS			
2a. SECURITY CLASSIFICATION AUTHORITY		3. DISTRIBUTION/AVAILABILITY OF REPORT			
2b. DECLASSIFICATION/DOWNGRADING SCHEDULE		Approved for public release; distribution is unlimited.			
4. PERFORMING ORGANIZATION REPORT NUMBER(S) NSWC TR 88-146		5. MONITORING ORGANIZATION REPORT NUMBER(S)			
6a. NAME OF PERFORMING ORGANIZATION Naval Surface Warfare Center	6b. OFFICE SYMBOL (If applicable) K23	7a. NAME OF MONITORING ORGANIZATION			
6c. ADDRESS (City, State, and ZIP Code) 10901 New Hampshire Avenue Silver Spring, MD 20903-5000		7b. ADDRESS (City, State, and ZIP Code)			
8a. NAME OF FUNDING/SPONSORING ORGANIZATION	8b. OFFICE SYMBOL (If applicable)	9. PROCUREMENT INSTRUMENT IDENTIFICATION NUMBER			
8c. ADDRESS (City, State, and ZIP Code)		10. SOURCE OF FUNDING NUMBERS			

10. SOURCE OF FUNDING NUMBERS			
PROGRAM ELEMENT NO.	PROJECT NO.	TASK NO	WORK UNIT ACCESSION NO.

11 TITLE (Include Security Classification) Graphite Heating Element Thermal and Structural Performance in the NSWC Hypervelocity Wind Tunnel 9--A Finite Element Analysis

12. PERSONAL AUTHOR(S) Metzger, Michael A.

13a. TYPE OF REPORT Final	13b. TIME COVERED FROM _____ TO _____	14. DATE OF REPORT (Year, Month, Day) 1988 June	15 PAGE COUNT 78

16. SUPPLEMENTARY NOTATION

17	COSATI CODES		18 SUBJECT TERMS (Continue on reverse if necessary and identify by block number)
FIELD	GROUP	SUB-GROUP	
13	01		SEE REVERSE
20	11		

19. ABSTRACT (Continue on reverse if necessary and identify by block number)

A general finite element based method for investigating the electrical, thermal, and themostructural performance of electrically powered heating devices is presented. The method is used to investigate the performance of a graphite heater configuration utilized in the NSWC Hypervelocity Wind Tunnel Facility (No. 9) for heating nitrogen gas to temperatures up to $3100°F$ prior to a tunnel run to prevent condensation of the gas during tunnel operation. The graphite heaters presently have a limited and erratic service life--a newly installed heater may fail after only 1 or as many as 100 or more tunnel run cycles. Electrical, thermal, and thermostructural performance data are presented for two graphite heater configurations. The thermostructural model is shown to correctly predict brittle fracture at fillet locations in the heater body where, in fact, most fractures are known to occur. Two methods for reducing fillet stresses are proposed which, if implemented, could substantially increase the useful service life of the graphite heaters.

20 DISTRIBUTION/AVAILABILITY OF ABSTRACT ☐ UNCLASSIFIED/UNLIMITED ☒ SAME AS RPT ☐ DTIC USERS	21. ABSTRACT SECURITY CLASSIFICATION UNCLASSIFIED	
22a NAME OF RESPONSIBLE INDIVIDUAL Michael A. Metzger	22b TELEPHONE (Include Area Code) 202/394-2063	22c. OFFICE SYMBOL K23

18. Cont.

Graphite	Heating elements	Brittle fracture
Brittle Failure	Failure Theory	Fracture
Maximum Normal Stress	Hypersonic	Wind Tunnel
Thermal-electric analogy	Electrical	Finite element
Hypervelocity	Crack	Nitrogen
Refractory	Probability	Thermostructural
Fatigue	Heat transfer	Stress
Strain	Voltage	Temperature
Thermal Stress/strain	Heat flux	Resistance Heating
Joule Heating	Convection	ABAQUS
PATRAN	Principal stress	Current
Current Density	Radiation	Conductivity
Resistivity	Free Convection	Tensile strength
Thermal Expansion	Service life	
Strain-to-failure		

FOREWORD

This report documents an investigation of the electrical, thermal, and thermostructural performance of graphite heating elements used in the Naval Surface Warfare Center (NSWC) Hypervelocity Wind Tunnel No. 9. This study is part of a larger and ongoing effort by the Aerodynamic Facilities Branch (Code K23) to reduce or eliminate the problem of frequent and costly failures of the graphite heaters. The analysis herein focuses on the nitrogen preheating period of the tunnel run cycle during which most heater failures are known to occur.

A general finite element-based method for investigating the performance of electrically powered heating elements is presented. The technique is applied to the Tunnel No. 9 graphite heater, and it is shown to correctly predict brittle fracture at fillet locations in the heater body where, in fact, most heater fractures occur. Two methods for reducing fillet stresses are proposed which, if implemented, could substantially increase the useful service life of the graphite heaters.

Accesion For	
NTIS CRA&I	✓
DTIC TAB	☐
Unannounced	☐
Justification	
By	
Distribution /	
Availability Codes	
Dist	Avail and / or Special
A-1	

Approved by:

R. Y. Schmidt

R. L. SCHMIDT, Head
Strategic Systems Department

iii/iv

CONTENTS

ILLUSTRATIONS

ILLUSTRATIONS (Cont.)

TABLES

CHAPTER 1

INTRODUCTION

The Naval Surface Warfare Center (NSWC) Hypervelocity Wind Tunnel No. 9 uses an electrically powered graphite heating element to preheat nitrogen working gas to temperatures up to 3100°F. This prevents condensation of the gas which cools as it expands through a nozzle to hypersonic speeds of Mach 10 or Mach 14. The graphite heater elements have a limited and erratic service life--a newly installed heater element may fail after only 1 or as many as 100 or more tunnel run cycles. Element replacement is costly (approximately $10,000 including installation), and a half day or more may be required to replace a broken heater element which adversely impacts the tunnel test schedule. This report documents a general method for investigating the electrical, thermal, and thermostructural performance of electrically powered heating elements. It also presents the results of an investigation of the heating characteristics of the Tunnel-9 graphite heater elements. This study was initiated to determine if thermal stresses induced in the heater elements during the nitrogen preheating period could be the cause of the heater element failures.

BACKGROUND

Tunnel-9 Operation

The NSWC Tunnel-9 wind tunnel is a "blow-down" type tunnel which runs at Mach 10 or 14. High pressure vertical heater and driver vessels (shown in Figure 1) are precharged with nitrogen gas prior to a wind tunnel run while a vacuum sphere downstream of the test section is evacuated. The fixed volume of gas in the heater vessel is preheated to the extreme temperature required. A tunnel run is initiated by bursting a set of metal diaphragms located just upstream of a 40-foot long nozzle which allows the high-pressure, high-temperature nitrogen (typically 20,000 psi at 3100°F for Mach 14) to accelerate through the nozzle section and reach speeds of Mach 10 or 14 in the 5-foot diameter test section. Relatively cool driver vessel gas pushes the hot gas out of the heater vessel under constant pressure to maintain constant flow conditions in the test section during the tunnel run. The tunnel run continues until all of the hot gas has been expended, a typical run lasting approximately from .25 second to as long 10 seconds.

The heater vessel (shown in Figure 2) is lined with a refractory insulation liner which safely contains the nitrogen gas during the preheating process. The liner encloses the graphite heater element which heats the nitrogen precharge to the specified final temperature of 1500°F (for Mach 10) or 3100°F (for Mach 14). This heating process is depicted in Figure 3. During the heating period, which lasts about 15 minutes, a 60 Hz, single phase ac current of 5500-6500 rms amps is passed through the hairpin-shaped graphite heater element which reaches a temperature of 4000-5000°F as a result of resistance heating. The nitrogen gas, which is essentially transparent to radiation, is heated primarily by convection and conduction off the hot graphite element and hot liner walls. Since the volume of nitrogen in the heater vessel is fixed, both its temperature and pressure rise during the constant volume heating process until the final desired pressure and temperature are reached. At this point the tunnel flow is started by rupturing the metal sealing diaphragms.

Heater Element Breakage Problem

Service life histories for heater elements used during FY 1985 and 1986 are shown in Table 1. A heater element is typically operated until it fails "catastrophically," usually by fracturing completely through one of the heating legs as shown in Figures 4 and 5. The timing and mode of failure are fairly consistent. The element usually fails completely at some point during the nitrogen heating period. The fracture is always a brittle-type fracture typically located at either a top fillet or bottom fillet (as shown in Figure 6) with the crack surfaces oriented approximately perpendicular to the longitudinal axis of the heater element.

Interestingly, it is now fairly well documented that a heater may develop partial cracks at the top or bottom fillets (as shown in Figures 7 and 8) which, at least for a time, will not adversely affect the heater operation. However, eventually the element fails completely and must be replaced. Although complete element failure occurs during the heating period, it is not clear if a partial crack is initiated at this or some other time.

Other work has been done to try to improve heater element life. Results of an investigation of thermal stresses, induced by quenching of the heater as the cool driver gas fills the heater vessel during a tunnel run, did not correlate well with Tunnel-9 experience. In another study, graphite material samples taken from both long-lived and short-lived failed heater elements were tested in an attempt to correlate service life with certain, easily obtained, non-destructive test measurements which could then be used as a quality control criterion for screening out unacceptable graphite material billets; however, no definite correlations were found.[1]

2

The present study is concerned with determining if thermal stresses induced in the heater elements during the nitrogen preheating period could be the cause of heater element failures.

CHAPTER 2

GENERAL HEATER ELEMENT PERFORMANCE ANALYSIS PROCEDURE

ANALYSIS PROCEDURE

The heater analysis procedure can be broken down into three basic steps:

Step 1: <u>Solve the Electrical Problem</u>--Get volumetric resistance heating in the graphite heater generated by a (5500 amp) current flow through the heater.

Step 2: <u>Solve the Thermal Problem</u>--Use internal heating from Step 1 to "heat up" the graphite element and obtain graphite temperatures.

Step 3: <u>Solve the Structural Problem</u>

o Use temperatures from Step 2 to obtain thermal stress and strain in heater due to thermal expansion. Determine maximum principal stress and strain in the heater.

o Subtract the hydrostatic stress or strain (generated by the high-pressure nitrogen gas surrounding the heater) from the peak principal stress or strain to obtain the net maximum principal stress or strain.

o Compare net maximum principal stress or strain with graphite strength to determine the probability of failure.

The entire three-step procedure above was implemented using the ABAQUS[2] Finite Element Analysis software (version 4-5) in conjunction with the PATRAN[3] pre- and post-processing code. The implementation of each of the three steps is described in more detail below.

Electric Resistance Heating--Step 1

Implementation of Step 1, that is, obtaining the volumetric resistance heating (also known as joule heating) due to the electric current passing through the graphite heater element, required a novel application of the well documented thermal/electric (T/E) analogy principal.[4] The T/E analogy has been widely used to solve analogous engineering problems in the fields of heat conduction, fluid dynamics, and solid mechanics. Phenomena which are governed by the Laplace equation, such as both electrical and heat conduction, yield mathematically identical solutions; the solution of a particular electrical conduction problem is also applicable to the corresponding or analogous heat conduction problem and vice versa. Analogous mathematical terms for the T/E analogy are given below:

THERMAL	ELECTRICAL
Heat, Q	Charge, Q
Temperature, T	Voltage, V
Heat Flux Vector, q	Current Density Vector, j
Thermal Conductivity, k	Electrical Conductivity, s

The typical approach to applying the T/E analogy has been to obtain a solution to a particular heat conduction problem using an analogous electrical conduction model (e.g., electrolytic tanks or conductive sheet models). In the present analysis, however, the opposite approach has been taken; that is, the electrical conduction in the heater is obtained by solving the analogous heat conduction problem using a geometrically similar finite element heat conduction model.

The ABAQUS thermal conduction capability can be utilized to easily solve for current flow in an arbitrarily shaped conductor subjected to some prescribed voltage. Since ABAQUS does not "know" that it is solving an analogous electrical conduction problem, it will state the results as "temperatures" and "heat-flux," etc. However if consistent analogous electrical terms are input, the "temperature" and "heat-flux" results from ABAQUS will actually be voltage and current-density, respectively. For this analysis, the units used for the input quantities were inches, volts and, for electrical conductivity, 1/ohm-in which produce units of volts and amps/sq in for the voltage and current-density output quantities, respectively. ABAQUS will calculate the components and also the magnitude of the current-density vector, j, at each gauss point in the finite element model. The volumetric resistance heating at each gauss point can then be obtained by Equation (1):

$$q = |j|^2 p \tag{1}$$

where: q = volumetric heat flux (watts/cu in)
$|j|$ = current density magnitude (amps/sq in)
p = electrical resistivity (ohm-in)

This last step of calculating the heat flux at each gauss point is done by running a short Fortran program I2RFIL (listed in Appendix A). This program simply reads the current density values from the ABAQUS results (FIL) file and generates a file of volumetric heat flux at each gauss point using Equation (1). This file of heat flux values is then used to heat-up the graphite element (Step 2 in the analysis procedure) to obtain the temperature in the heater.

<u>Limitations of T/E Method</u>. There are two principal limitations in the T/E method described above. First, the electrical conductivity must remain constant with temperature. Although ABAQUS will handle temperature dependent <u>thermal</u> conductivity, this capability cannot presently be utilized for temperature dependent <u>electrical</u> conductivity since the actual temperatures are not known in Step 1. They are computed later on during Step 2 in the analysis procedure. As Figure 9 shows, the electrical resistivity (the resistivity is simply the inverse of conductivity) of the graphite material is strongly temperature dependent up to about 1400°F, then remains fairly constant at temperatures above this. It was found that the heater element legs run at temperatures above this, except for the initial heat-up period, which lasts about a minute, so that for most of the 15-20 minute nitrogen heating period the electrical conductivity can be taken to be uniform and constant.

This method is also in a strict sense limited to dc electrical power. Recall that the Tunnel-9 heater elements are powered by a 60 Hz, ac power source. An ac current produces a so-called "skin effect" which causes a concentration of the current density at the outer surface of a conductor rather than being uniformly distributed through the cross section as in dc current flow. This effect is proportional to the ac frequency and size of the conductor and is inversely proportional to resistivity. It was determined that, in regard to the volumetric heating, this effect would be secondary for the graphite heater elements so that the dc current flow analogy should adequately model the heating characteristics.

Graphite Element Heating--Step 2

Since both Steps 1 and 2 in this analysis procedure use a heat conduction finite element model, the basic model used in Step 1 can be used in Step 2 with changes in the boundary conditions to reflect the new nature of the problem. ABAQUS is capable of solving very general transient and steady-state heat transfer problems involving internal heat generation, radiation, and convection with temperature dependent properties.

Recall from Figure 3 that once power to the heater is turned on at the start of the heating period, the graphite element heats up in about 1 minute. During this time the temperature of the

nitrogen gas in the heater vessel does not increase appreciably. For analysis purposes this initial heating transient must be viewed as a nonsteady-state phenomenon. After about 1 minute, the heater element temperature reaches a nearly steady-state level and, thereafter, both the heater and nitrogen gas temperatures rise slowly for the remaining 15-20 minutes of heating time. For analysis purposes this relatively slow heating process can be treated as a quasi-steady state process so that the heater temperature can be assumed to be a function solely of the surrounding gas/liner-wall temperature. The problem of obtaining the temperature distribution in the heater at any point during the quasi-steady heating reduces to simply fixing the gas/wall temperature and solving for the steady-state heater temperature distribution. Since performing a transient analysis is in general much more costly, it was decided to limit the present study to investigating the heater temperatures and stresses at selected points in time within this quasi-steady heating period. The two points selected for study were at the start and end of the quasi-steady heating period and which are designated as "START HEAT" and "END HEAT" in Figure 3. Additionally, the gas and liner-wall temperatures were assumed to be identical permitting the use of one sink temperature for both radiation and convection boundary conditions.

Obtaining the temperature distribution in the graphite heater at the START or END HEAT is a matter of specifying the proper sink temperature in ABAQUS, as well as specifying radiation and convection heat transfer coefficients, and then allowing ABAQUS to solve for the steady-state temperatures in the heater due to the resistance heating provided by Step 1. Since the resistance heating in the heater is non-uniform, the ABAQUS subroutine option DFLUX is used with the subroutine given in Appendix A to read the heating flux values from the file generated in Step 1. ABAQUS calculates the temperatures in the heater which are then used to evaluate thermal performance of the heater and to obtain thermal stresses in the heater.

Graphite Element Thermal Stresses--Step 3

Once again the same basic finite element model from Steps 1 and 2 can be used in Step 3 if the element type designator is changed to the corresponding solid structural element. ABAQUS will then use the temperatures obtained from Step 2 to compute the thermal stresses and strains in the graphite heater element. A suitable failure criteria can then be applied to the stress or strain results to determine probability of failure or assess margins of safety of the heater design.

PRACTICUM

In practice, implementation of this three-step analysis procedure involves additional work, primarily in Step 1, to

8

ensure that correct results are obtained. Table 2 summarizes the semi-automated steps for the entire procedure as implemented on a VAX computer system. In Step 1 the user specifies a heater voltage and ABAQUS solves for current flow. The current checking program CURRENT (Appendix A) will verify that the net current flow through the heater is correct. If it is not, then the applied voltage may be adjusted. Once the correct net current is obtained, the program I2RFIL (Appendix A) is run which creates the resistance heating file (FOR032.DAT file) from the ABAQUS results file. Once the heating file is generated, it should be checked by running the POWER program (Appendix A) which calculates the total heater power that will be generated by the heating file. The total power calculated by POWER should be within a few percent of the specified heater voltage multiplied by the total heater current computed by CURRENT (i.e., the total resistance-heating power should equal applied heater volts times total amps). Some discrepancy can be expected since the algorithm used in POWER to compute finite element volumes is not exact for quadratic elements with curved edges.

CHAPTER 3

PERFORMANCE ANALYSIS RESULTS FOR TUNNEL-9 GRAPHITE HEATING ELEMENTS

ANALYSIS RESULTS

The two most current graphite heater element configurations, hereafter referred to as the J-type and K-type heaters, are shown in Figure 10 and 11. The drawing for the Mach 10 heater base is shown in Figure 12. The K heater has superceded the J heater, the differences being in the flared top and the side slots. In the K design, the slight flare-out of the outer diameter at the top end was lengthened, and the slot was also lengthened in order to "beef-up" the top fillet region where the earlier J-type heaters tended to break. This change appears to have reduced top fillet breaks but, unfortunately, the K heaters continued to fracture at the bottom fillet. Both the J and K heaters were analyzed with the basic finite element models shown in Figure 13 and 14. Both are 1/4-symmetry models utilizing the two planes of symmetry in the heater to reduce model size as shown in Figure 15. The J model is a full-length model, whereas only the top portion of the K design was analyzed. Extensive studies showed that such top models would give the same stress results as the full model when out-of-plane motion of the cross section at the cutoff is prevented. Quadratic finite elements were used in both the thermal models and the stress models (20-node hexes and 15-node wedges, ABAQUS DC3D20- and C3D20-type elements, respectively). The Mach 10 graphite heater base, which holds the heater element, was also analyzed separately using the 1/4-symmetry model shown in Figure 16. Only the bottom portion of the heater element, up to the bottom fillet region, is included in the base model. The results of the base analysis will not be discussed extensively in this report--these results are presented for reference.

Electrical Analysis Results--Step 1

Results for voltage and current density distributions in the J-type heater are shown in Figure 17 and 18, respectively. The current density plot can be viewed as a topographical map with peaks showing regions of high current densities, such as at both the top and bottom fillets, and valleys indicating areas of relatively low current densities. The ABAQUS material and boundary conditions are given in Appendix B for the J heater electrical model.

Thermal Analysis Results--Step 2

Thermal Model Setup. In all cases convection heat transfer was allowed on the inner diameter (I.D.) and outer diameter (O.D.) "wetted" surfaces of the heater element as well as on the rounded end of the crown and edges of the side slots. The O.D. and I.D. of the threaded-base portion of the J heater was fixed at 300°F. Radiation heat transfer was allowed on the wetted O.D., slot edges, and the rounded end of the crown. No radiation was allowed on the wetted I.D. since the inside surfaces of the heater element legs face each other so that the net radiation to each surface is taken to be zero as a first approximation. Table 3 lists the film coefficients and radiation boundary conditions used. ABAQUS input data for the J thermal model are given in Appendix B, and Appendix C shows the method used to compute the free convection film coefficient.

Thermal Results. Figures 19-23 show temperature results for the three models analyzed. Figures 19 and 20 show temperatures in the J heater for a standard 613 kW power case (5481.8 A @ 112 V) for both START HEAT and END HEAT periods. The peak temperatures in the graphite are 3620°F at START HEAT and 4858°F at END HEAT, and they occur at the "hotspot" apparent on the I.D. surface near the top fillet. Cross-sectional temperature profiles at the top and bottom fillets for the END HEAT case (Figure 21) reveal internal hotspots at both fillet locations corresponding approximately to the locations where the high current densities occur. Also readily observed in these plots is the hot core along the inside center of the heater element leg which is undoubtedly due to the lack of radiation cooling on the I.D. of the heater leg. An END-HEAT case was run at 913 kW (6680 A) which resulted in an increase of peak temperature to 5622°F. No experimental data were available at this time to correlate with these temperature results.

Figure 22 shows the temperature results for the K heater which was run only at the START HEAT condition. The graphite base model results are shown in Figure 23. The base results shown in Figures 23 and 24 are for a slightly higher heater power of 653 kW.

Thermostructural Analysis Results--Step 3

Although the heater element is clamped to the graphite base with set screws (as shown in Figure 25) both clamped and free heater element leg end-fixity conditions were analyzed to study the effects of end- fixity on stresses. ABAQUS input data for the clamped-base J model are given in Appendix B. Figure 26 and 27 give highly exaggerated deformation plots showing both the clamped- and free-end results. The fact that the heater element leg deflects inward at the free end is probably due to the

relatively cool edges of the heater element leg, which do not grow by thermal expansion as much as the hotter center portion, and tend to pull or warp the center toward the edges.

Since it is known in advance that the heater elements fail by brittle fracture at the top and bottom fillets and that the fracture plane is approximately perpendicular to the heater element longitudinal axis, one might expect to find high axial tensile stresses at these fillet locations if, indeed, the thermal heating stresses are the cause of heater failures. The plots of axial stress in Figure 28 in fact show peak tensile stresses of 6896 and 7046 psi occurring in the J heater at the top and bottom fillets, respectively, for START HEAT. The axial stress distributions in the K heater and the heater base are shown in Figures 29 and 24. An assessment of heater element failures, based on these stress results, is given in the following two sections.

Failure Analysis--Stress Based. For brittle-type fractures in an isotropic material the so-called "maximum normal stress" failure theory can be used as the failure criterion.[5] This theory states that <u>tensile fracture will occur when the maximum tensile principal stress exceeds the tensile ultimate strength of the material</u>. The (algebraically) maximum principal stress plots for the J and K heater and the heater base are shown in Figures 30-34 (Figure 35 is discussed on page 16). Peak tensile principal stresses at START HEAT of 7000 psi* occur at the fillets in the J heater in Figure 30, but the K heater in Figure 33 shows a relatively low stress at the fillet and a relatively low peak stress at the center of the leg of 4124 psi. Table 4 lists the state of thermal stress and strain at each gauss point in the top and bottom fillets where the highest principal stress occurs. As shown in Table 4 by the "axial tilt" angles of 6-19 degrees, these principal stresses act approximately in the axial direction as expected.

High axial principal stresses also occur at the threaded base of the heater element where it necks down to the thinner wall, and they are especially noticeable for the END HEAT cases (both clamped and free) in Figures 31 and 32. Failures in this base region are fairly rare, however, indicating that perhaps there is some give at the base/heater interface which limits these stresses.

The principal stress profile in the graphite near the surface of the fillets can be seen in Figures 36 and 37. These figures show profiles of temperature and the total principal

---

*The axial fillet stresses in Figure 28 are "nodal averaged" results whereas the principal stresses in Figure 30 were manual extrapolations to the fillet surfaces of more accurate gauss point data. The use of two different extrapolation methods accounts for the predicted bottom fillet axial stress being higher than the principal stress.

stress (the total principal stress is equal to the thermal stress minus the 750 psi compressive stress due to the hydrostatic pressure of the nitrogen gas which surrounds the heater). The stress reaches the maximum level at the fillet surface where both the temperature and the strength of the graphite are lowest. The strength of graphite, unlike most common engineering materials, actually increases substantially with increasing temperature up to about 5000°F. In both Figure 36 and 37, the stress at or near the fillet surface exceeds the indicated 4100 ksi tensile strength of the graphite indicating that a fracture is likely to occur in the fillets. This result correlates very well with the failures observed in the Tunnel-9 heater elements.

Failure Analysis--Strain Based. Table 4 lists the strains at the critical locations in the top and bottom fillets. Both the total strains and elastic strains are shown. The elastic strain (or "strain due to stress") is equal to the total strain minus the thermal strain component, $\alpha\Delta T$, at the point in question. This elastic strain value can be compared to conventional strain-to-failure data to assess probability of failure. Test data for strain-to-failure, taken from actual heater element graphite material, is shown in Appendix D. The data are for axial and circumferential directions at an elevated temperature of 2000°F, and they are plotted as strain versus probability-of-failure (POF). A POF of 60 percent, for example, means that 60 percent of the test samples failed at the indicated strain level. Profiles of total principal elastic strain in the top and bottom fillets are shown in Figures 38 and 39. As in the stress case, the maximum strain occurs at the fillet surface. The estimated maximum principal strains indicated in Figures 38 and 39 were obtained by increasing the axial strain by the principal to axial stress ratio at the point in question and then subtracting the hydrostatic strain[*] as shown here:

$$\text{principal strain} = \text{axial strain}\left(\frac{\text{principal stress}}{\text{axial stress}}\right) - \text{hydro. strain}$$

$$= .00319 \ (5815/5471) - .000326$$

$$= .00306 \ \text{in/in} \quad (@ \ \text{Top Fillet, GAUSS POINT 7})$$

The maximum principal elastic strains at START HEAT are .00375 and .00388 in/in in the top and bottom fillets, respectively, as shown in Figures 38 and 39. These strain levels correspond to a POF of 65 percent and 75 percent, respectively, which says 65 to 75 percent of the heater elements should fail relatively quickly, and that the remainder should have relatively long service lives. The actual heater element service lives shown earlier in Table 1 can be plotted statistically as service

---

[*] The hydrostatic strain, E_h, due to the 750 psi gas pressure is computed using: $E_h = (1-2v)P/E$ where E_h=hydrostatic strain, v=poisson ratio, P=pressure, E= Young's modulus.

versus percentage of heater elements which will fail by this life (cumulative frequency) as Figure 40 shows. Interestingly, the data show that up to about 70 percent of the heater elements had average (20 cycles) or shorter service lives, and about 20 percent had relatively long service lives of 50 or more cycles. This result agrees well with the strain based failure rate prediction, and this is somewhat fortuitous considering the small statistical population used and other factors. This result shows that, for a linear stress analysis such as this one, the strain based failure criterion yields more realistic results than the stress based one which, in all cases, predicts a 100 percent failure rate based on the data in Appendix D. This is due to the fact that graphite material exhibits a strain-softening stress-strain relation which, if ignored, will cause the thermal stresses to be over-predicted.

Table 5 summarizes the stress and strain failure analysis results. Note that even the strain failure rate is 100 percent for the high power (913 kW) case in Table 5 owing to the substantial increase in fillet stress with increased heater power. It has been found that, in fact, heater element failures occur more frequently when the heater elements are run at higher power levels.

GRAPHITE HEATER ELEMENT FILLET STRESSES

During the course of this investigation various studies were performed to:

1. Explain why high axial tensile stresses occur at the top and bottom fillets.

2. Investigate methods to reduce high stresses in the graphite heater elements, thereby providing a means to extend the useful service life of a heater element.

Fillet Stress Breakdown

Parametric studies were performed to breakdown the bottom fillet stress into component parts. Figure 41 presents the results of these studies. Five main effects are identified here in order of importance:

1. Differential Radiation Effect (42 percent)
2. Edge Cooling Effect (31 percent)
3. Thickness Cooling Effect (17 percent)
4. Beam Bending Effect (6 percent)
5. Fillet Hotspot Effect (4 percent)

Each effect is described below briefly.

Differential Radiation Effect. The O.D. of the heater tube radiates freely to the heater vessel liner whereas the I.D. is more or less enclosed; hence, there is a decreasing temperature gradient from the I.D. to the O.D., tending to induce axial tension at the O.D. and axial compression at the I.D.

Edge Cooling Effect. The edges of the heater element legs are more efficiently cooled than the center portion because of exposure to the cool nitrogen gas on three surfaces instead of just two. Hence the edges tend to stay at a lower temperature than the center and, due to less thermal expansion, are "stretched" axially by the hotter center and develop axial tensile stress.

Thickness Cooling Effect. Internal volumetric heating in a thin slab with cooling on the slab surfaces produces a parabolic temperature gradient. The core of the slab tends to expand more than the outer material creating a compressive core and tensile skin.

Beam Bending Effect. The gross thermal expansion of the heater element sets up "beam bending"-type stresses in the heater element legs when the base is clamped. The 6 percent figure indicated for this effect may be conservative since it is based on a case where the heater was uniformly heated to 4000°F which does not induce the more severe gross warping evident in Figure 26.

Hotspot Effect. Additional thermal expansion of material at the internal hot-spots located near the fillets tends to put additional tensile stress in the fillets.

The first three effects perhaps explain why the axial thermal stresses in the heater element leg are tensile at the O.D., even more tensile at the edges, and compressive at the center core. The last two effects may explain in part why the tensile edge stresses tend to peak out at the top and bottom fillets.

Stress Reduction Methods

Regarding the edge cooling effect, it was noticed in the course of these studies that the temperature in a heater element leg is lowest at the sharp corners on the edges of the leg (as shown in Figure 35). This cooler material cannot expand as much as the core and, hence, the corners are stretched in tension as the hot core expands. It was found that rounding off the sharp corners, as shown in Figure 35 and 42, substantially reduced fillet stresses on the order of 20 to 30 percent.

Another technique which may be useful for reducing fillet and edge tensile stresses is to provide a "cooling slot" at the center of each heater element leg to help cool the hot core. Figure 43 shows how this could be done by "slicing" the legs through at section AA and rotating the halves outward. A prototype design for such a heater element is shown in Figure 44 where the cooling slot extends the full length of the hot portion of the heater element leg. It was found in one analysis of a cooling slot design that the top and bottom fillet stresses decreased by 25 percent and 35 percent, respectively, as compared to the nonslotted heater element.

ASSUMPTIONS

Various assumptions were made in this analysis. For example, the use of one identical sink temperature for both convection and radiation heat transfer assumes the insulation liners run at the same temperature as the nitrogen gas. However, since nitrogen gas is essentially transparent to heater radiation, the liner receives radiation directly from the heater element and probably runs hotter than the gas. (Preliminary calculations indicate that the liner may run 800°F hotter.) This effect would lead to a hotter element and, as some preliminary analyses have recently shown, somewhat lower thermal fillet stresses in the heater element (perhaps 20 percent lower). On the other hand, although the fillet stresses may be lower, the true ultimate tensile strength of a given volume of graphite may be significantly lower than the average strength used here. This is due to the actual strength of a brittle material (such as graphite) being determined by the distribution of flaws in the material.[6] For this reason the tensile strength of graphite is highly variable to such a point that the true strength of any one sample can vary significantly from the average strength data. The statistical tensile strength plots in Appendix D were obtained from tensile tests on actual graphite samples which were machined from failed heater element material, and they show the scatter typical for this graphite. The statistical strength variation shown in Appendix D holds only for the specific volume of material associated with the tensile specimen gauge section (Vol = 0.066 cu in). In order to accurately assess failure in a graphite part such as a heater element, a sophisticated failure assessment must be carried out that accounts for the volume of material in the element which is subjected to high tensile stresses. A failure criterion with these features requires a large body of statistical material data which is currently not available for the heater element.[7]

CHAPTER 4

CONCLUSIONS

This report documents a general finite element method for investigating the electrical, thermal, and thermostructural performance of electrically powered heating devices. The method was applied to a graphite heater element utilized in the NSWC Hypervelocity Tunnel No. 9 to pre-heat nitrogen working gas to temperatures of 3100°F. Electric current density and temperature distributions at the start and end of the nitrogen preheating period are presented. Thermal stresses in the graphite heater element are presented which predict that crack initiation of the type actually exhibited in the heater elements is likely to occur at the top or bottom fillet of the J-type heater due to high tensile thermal stresses which occur in these regions. The likelihood of a crack starting is greater near the beginning of the heating period. Also, it is greater with lower Reynold's Number tunnel conditions since the relatively low hydrostatic pressure of nitrogen gas at these conditions does not relieve the tensile fillet stresses enough to prevent fracture. The results correctly predict that crack initiation is more likely at higher heater powers due to an increase in fillet thermal stresses with increased power. The stress models also correctly predict that the K-type heater will tend to fail at the bottom fillet because the geometry of the K heater at the top fillet effectively limits the axial tensile stress in the top fillet to relatively low levels.

Two methods for reducing fillet stress levels are presented. First, the technique of rounding the edges of the heater element legs is shown to reduce fillet stresses by perhaps 20 to 30 percent. Second, by providing a central cooling slot in each heater element leg, the fillet stresses were reduced by 25 to 35 percent.

The results presented here suggest that the fillet stresses generated during the nitrogen heating period are a primary cause of heater element fracture. The exact mechanism for initial fracture may be tensile fracture or fatigue. If high tensile fillet stresses during heating are in fact causing the heater element failures, then the two methods presented for reducing fillet and edge stresses, if implemented, may significantly increase the survivability of the Tunnel-9 graphite heater element.
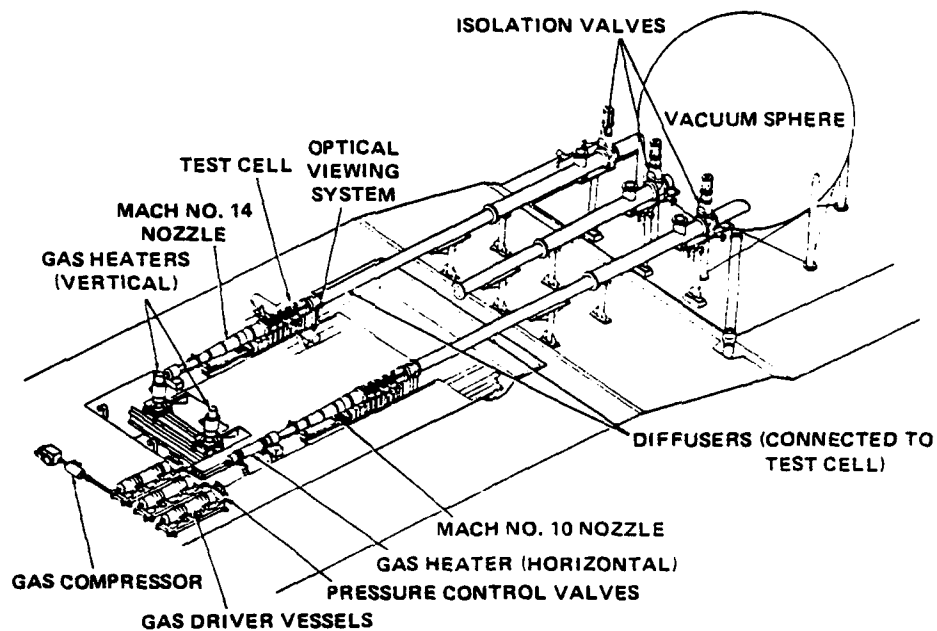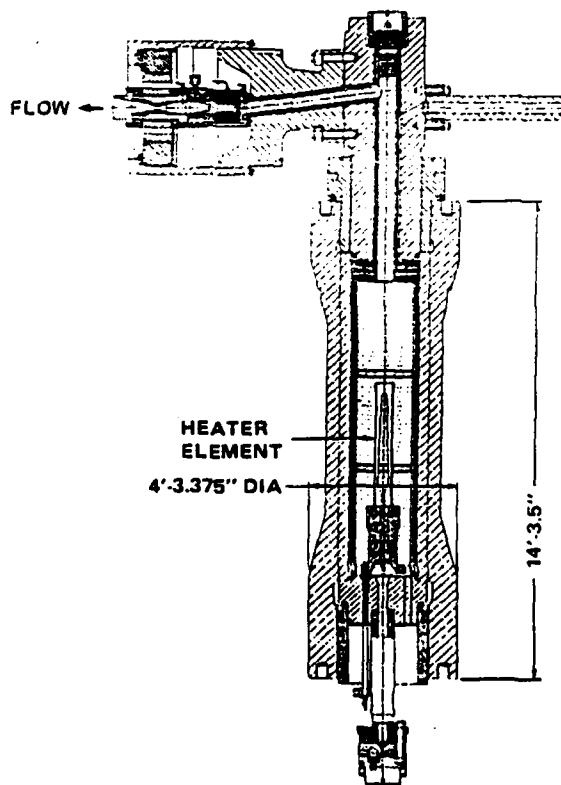
FIGURE 1. SCHEMATIC OF TUNNEL NO. 9 FACILITY

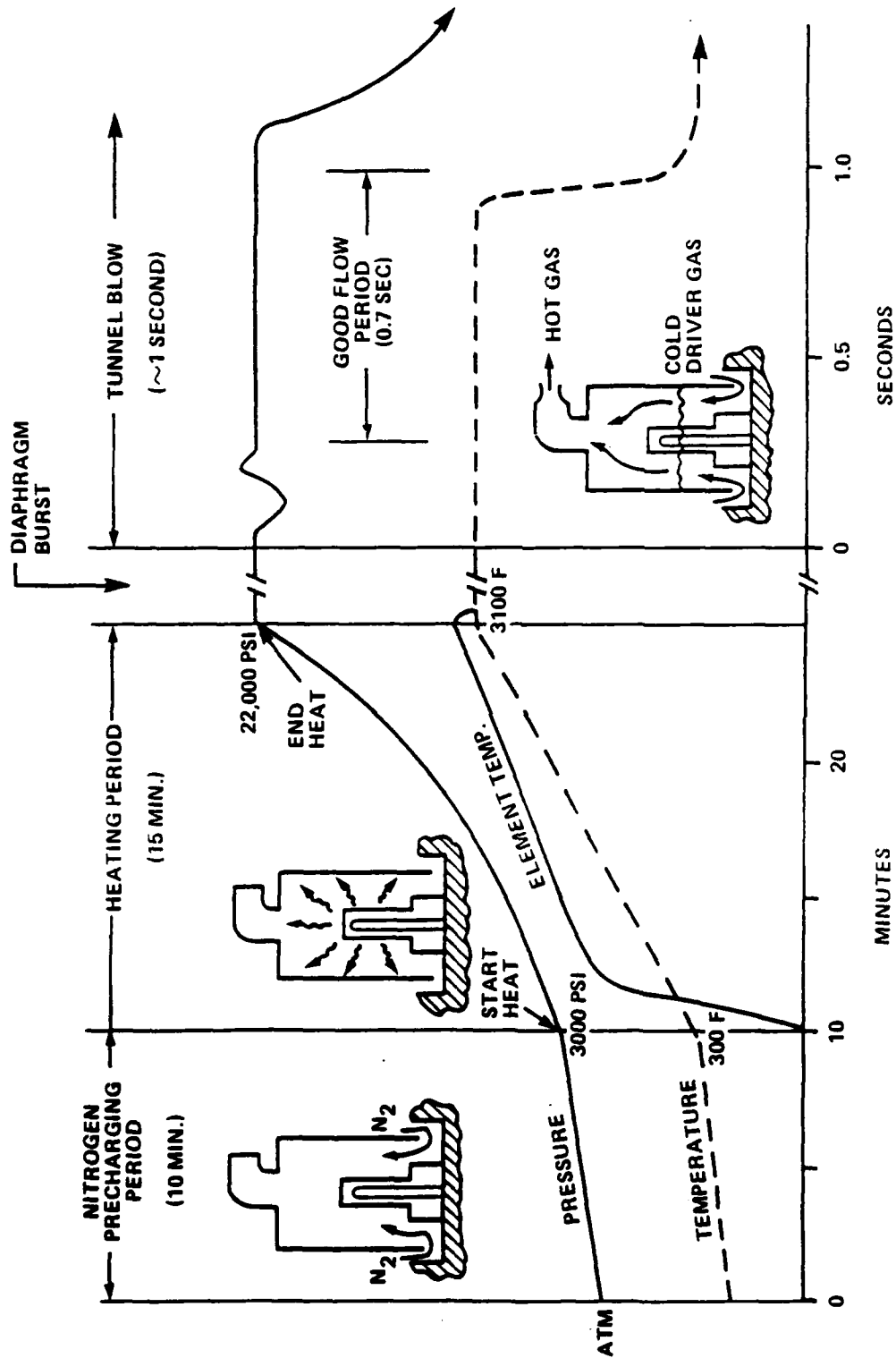FIGURE 2. VERTICAL HEATER AND DIAPHRAGM SECTION

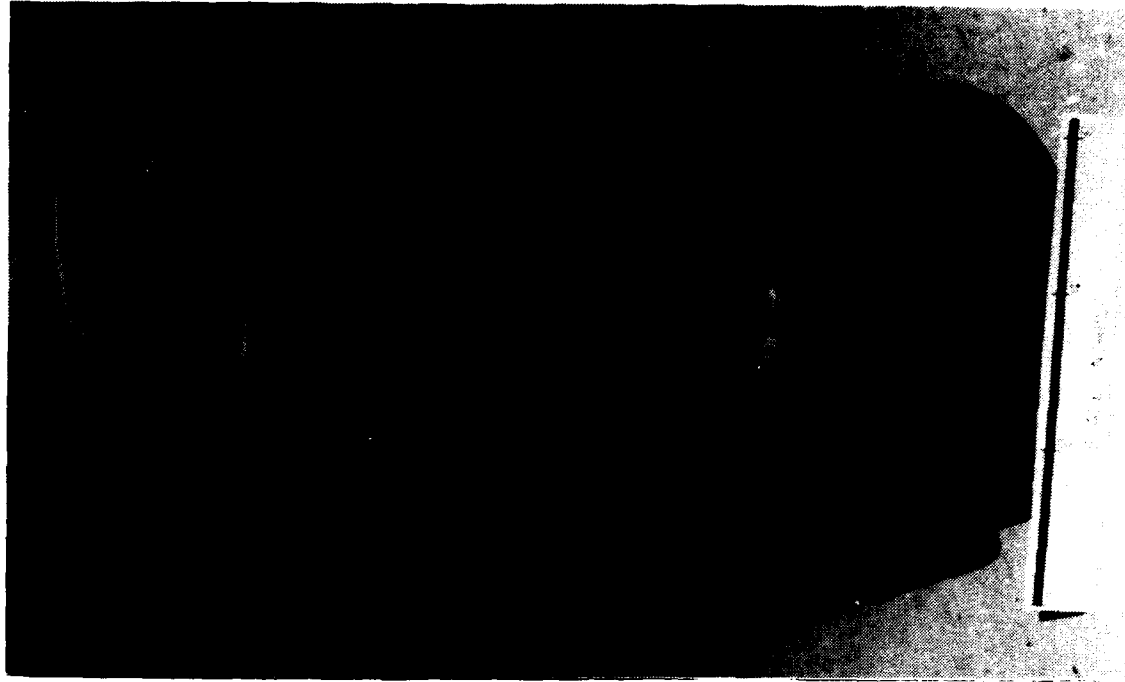FIGURE 3. HEATER GAS CONDITIONS FOR A TYPICAL MACH-14 WIND TUNNEL RUN

FIGURE 5. COMPLETELY FAILED HEATER – BOTTOM FILLET LOCATION

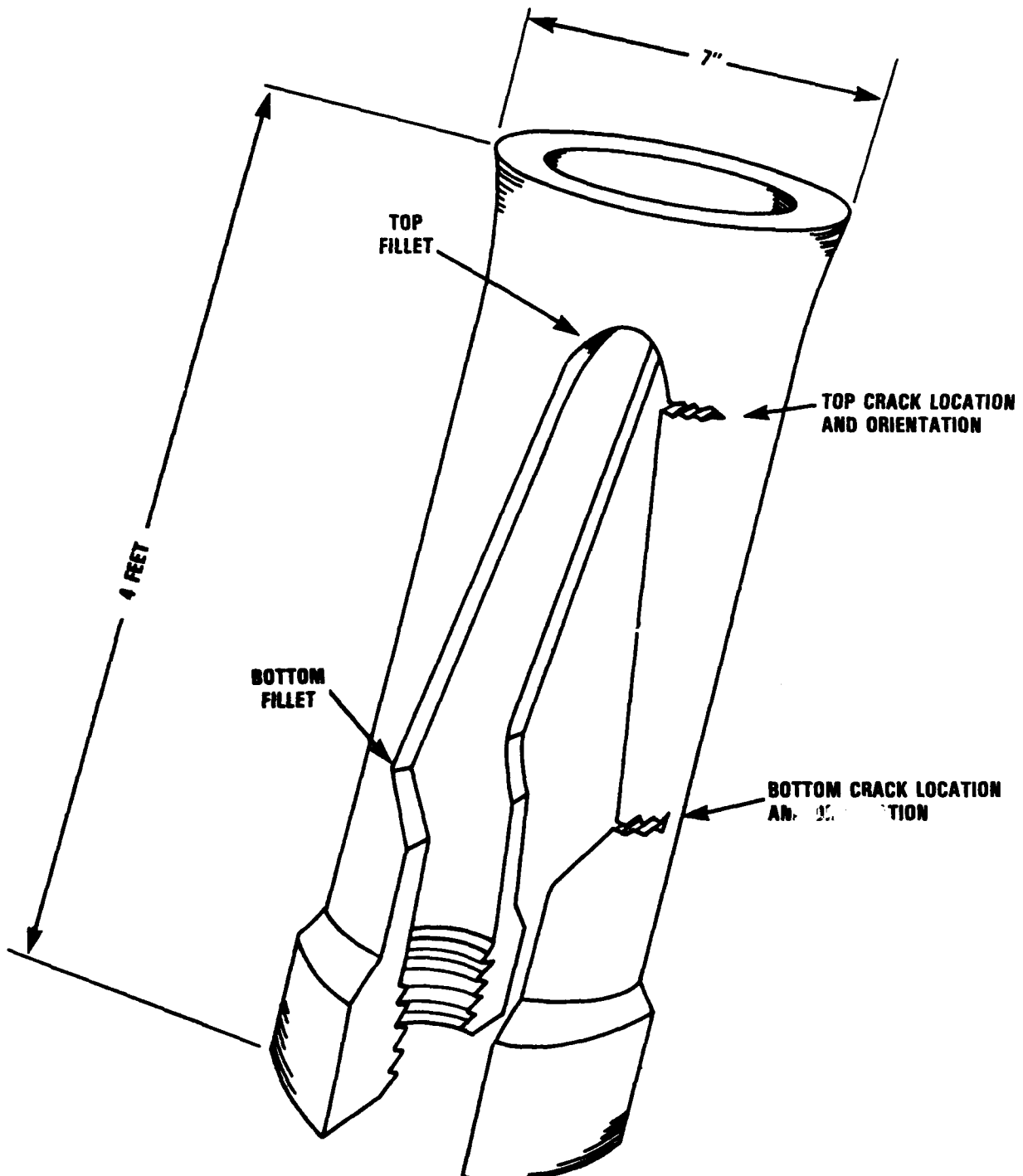FIGURE 4. COMPLETELY FAILED HEATER – TOP FILLET LOCATION

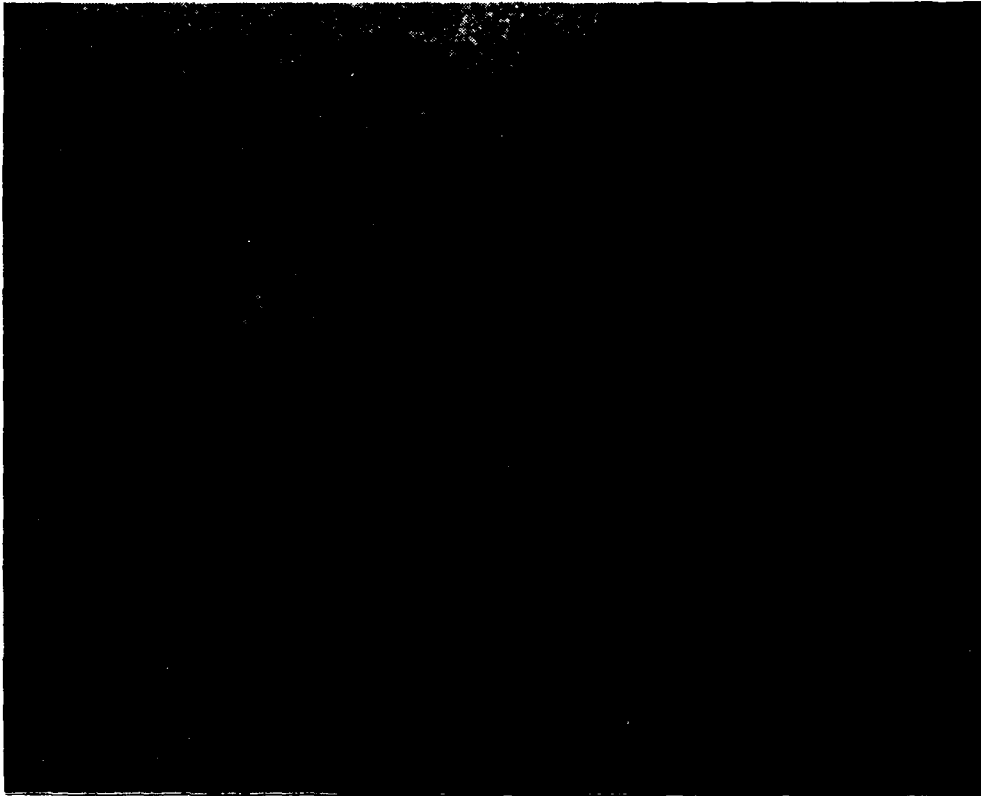**FIGURE 6. TOP AND BOTTOM FILLET CRACK LOCATIONS IN THE GRAPHITE HEATER**
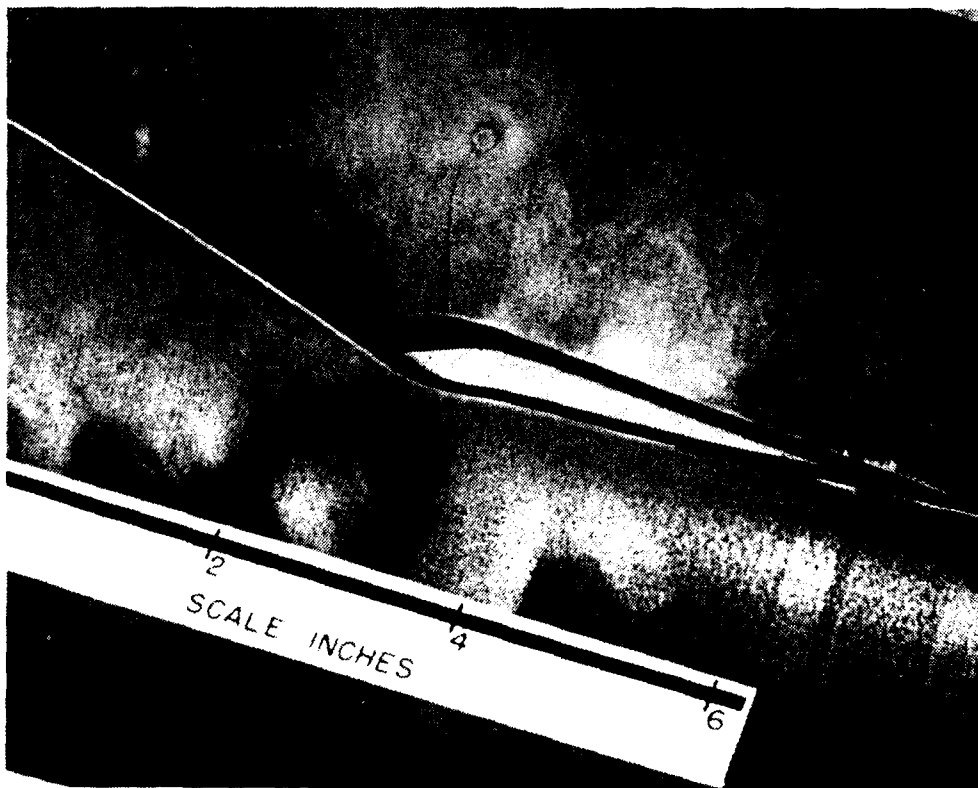
FIGURE 7. PARTIAL TOP FILLET CRACK

FIGURE 8. PARTIAL BOTTOM FILLET CRACKS

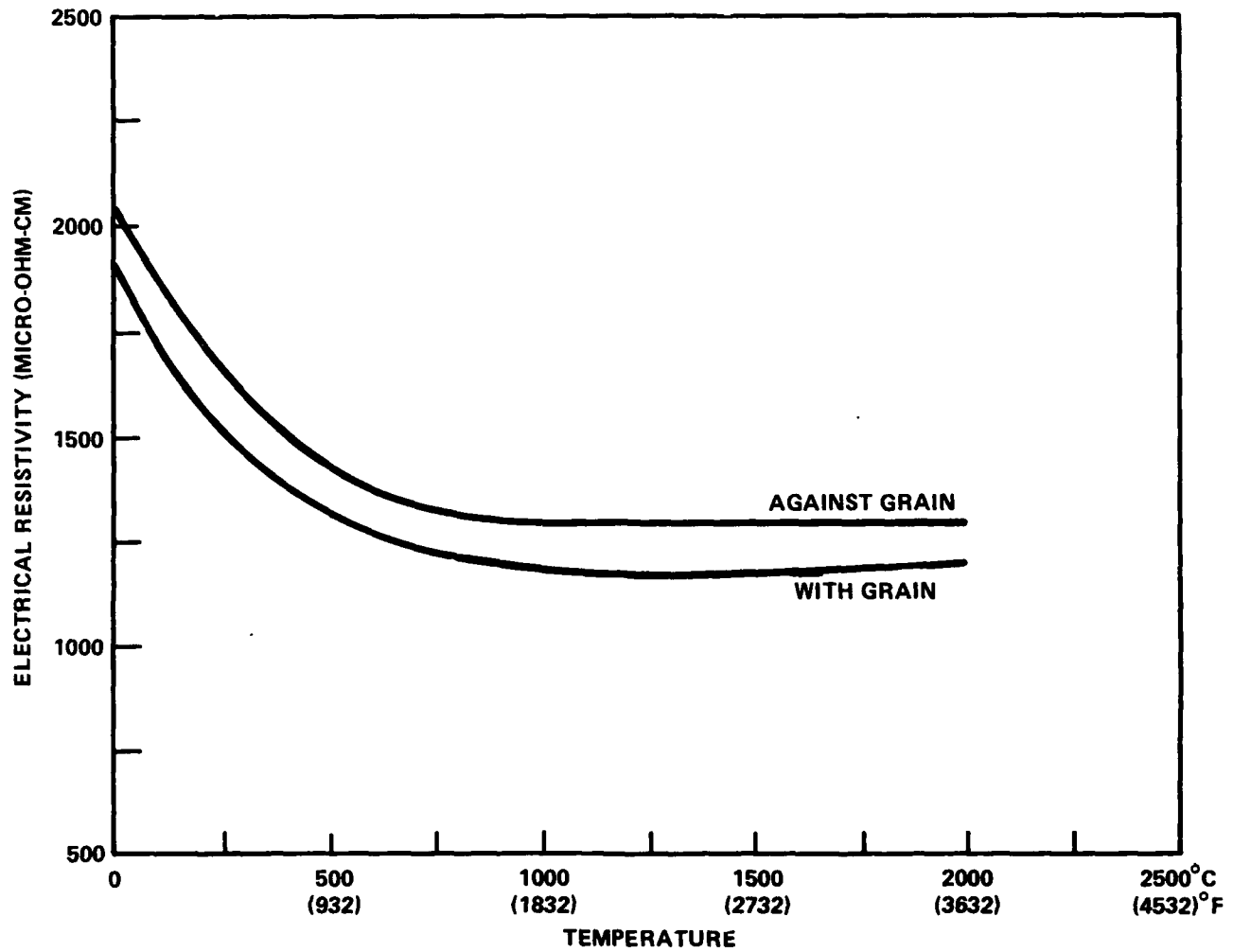FIGURE 9. HEATER GRAPHITE ELECTRICAL RESISTIVITY VERSUS TEMPERATURE

FIGURE 10. J HEATER DRAWING

FIGURE 11. K HEATER DRAWING

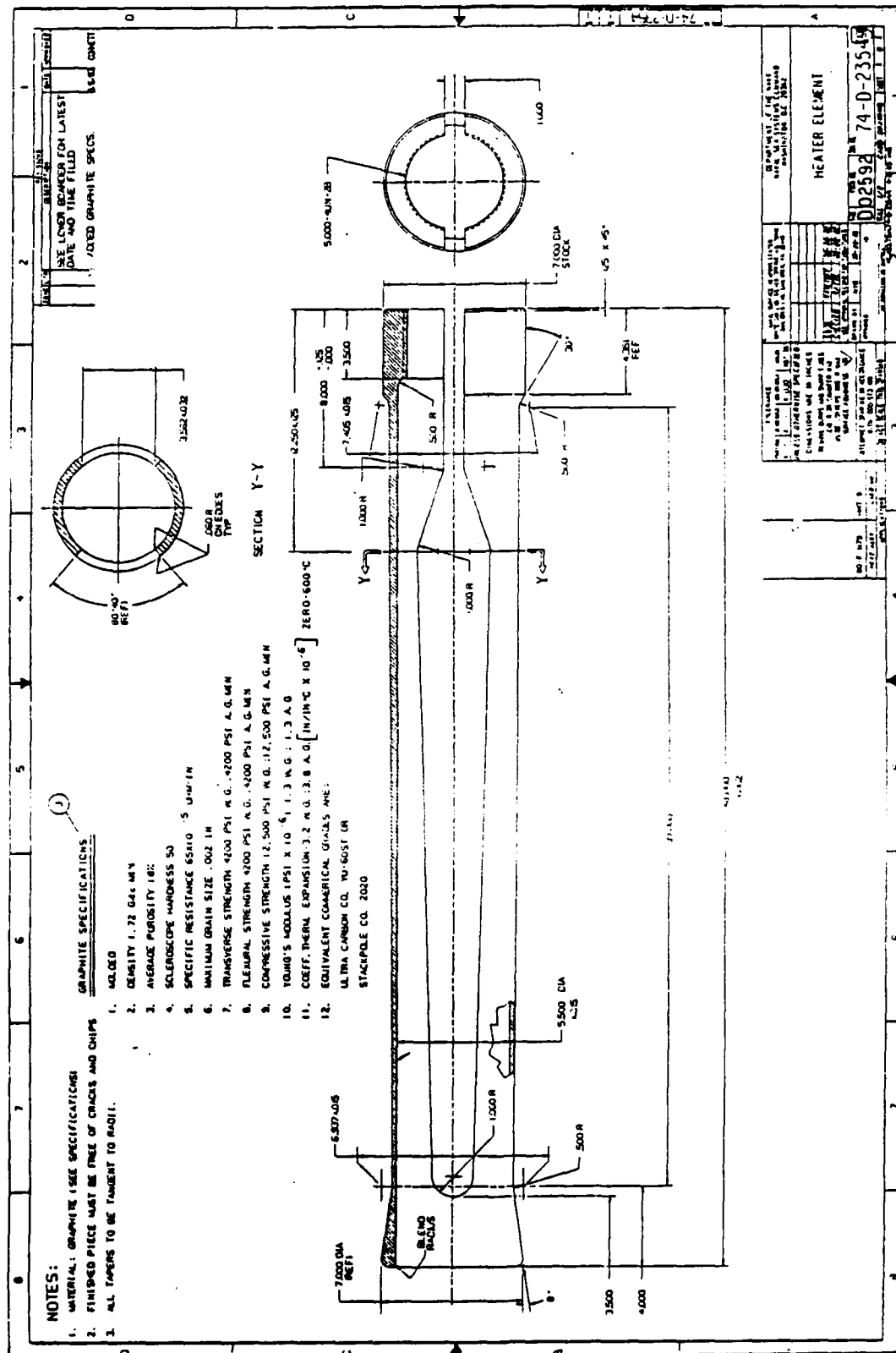FIGURE 12. MACH-10 HEATER BASE DRAWING
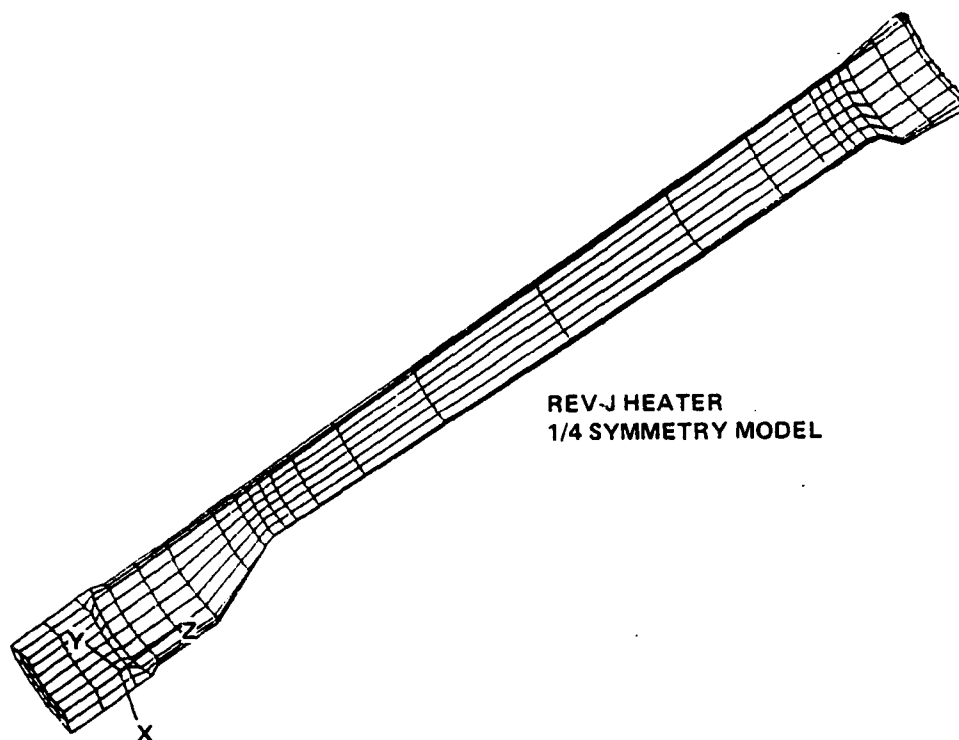
FIGURE 13. J HEATER FINITE ELEMENT MODEL
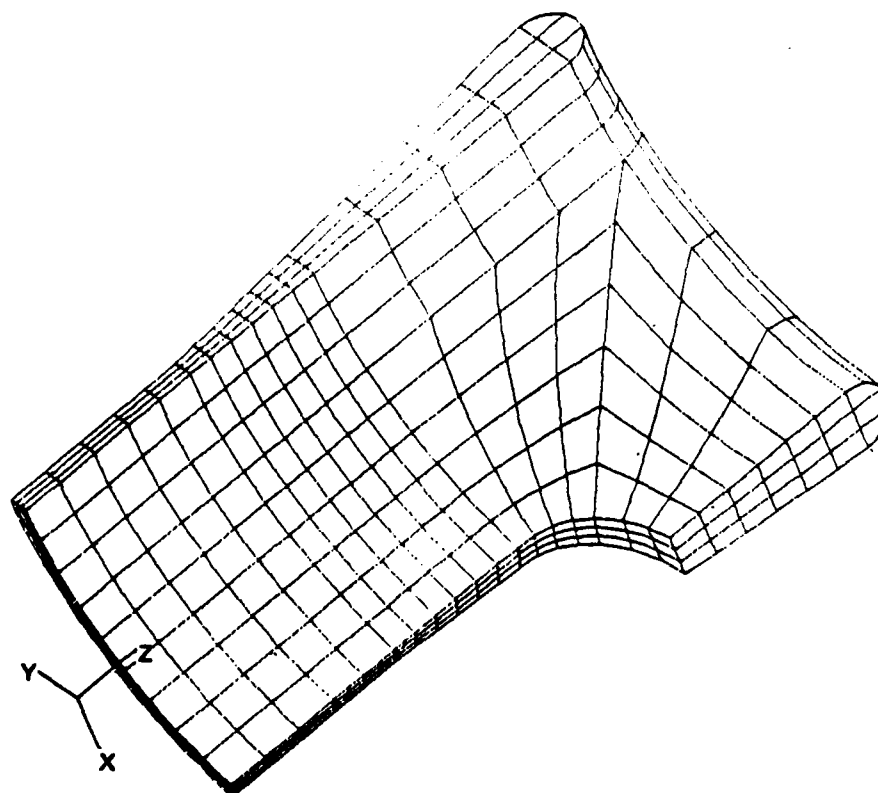
FIGURE 14. K HEATER FINITE ELEMENT MODEL

FULL MODEL   1/2 SYMMETRY MODEL   1/4 SYMMETRY MODEL
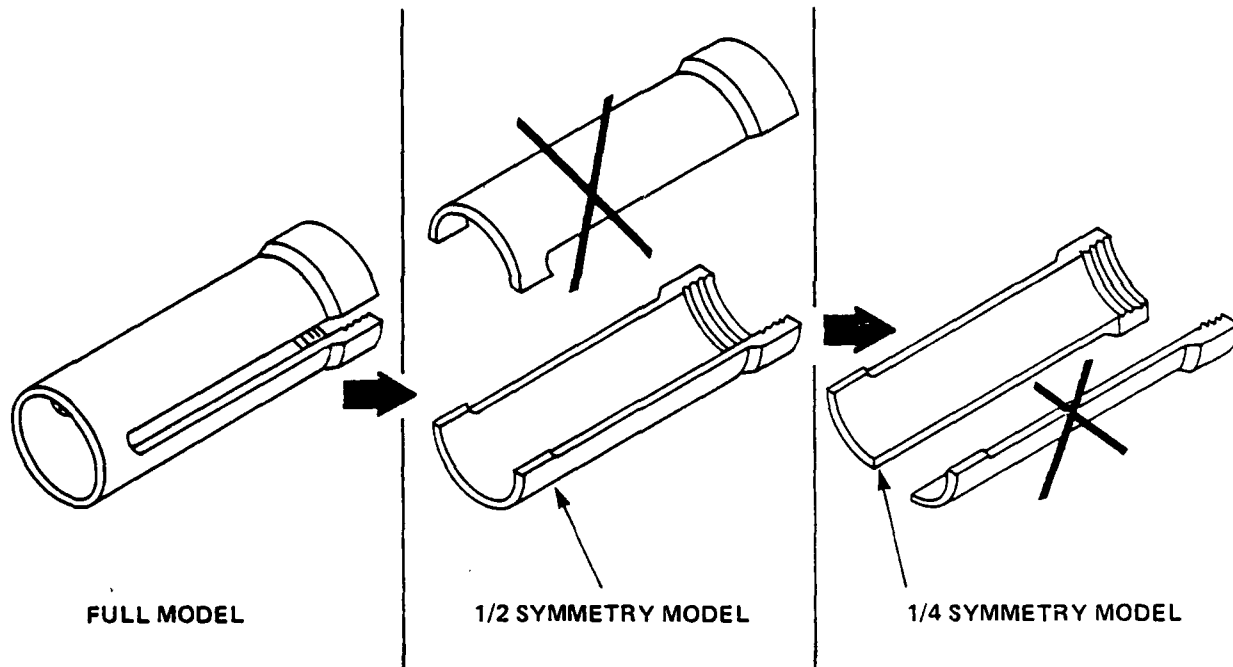
FIGURE 15. FINITE ELEMENT MODEL USES HEATER SYMMETRY TO REDUCE MODEL
SIZE

MACH-10 HEATER BASE + REV-J/K GRAPHITE HEATER
1/4 SYMMETRY MODEL
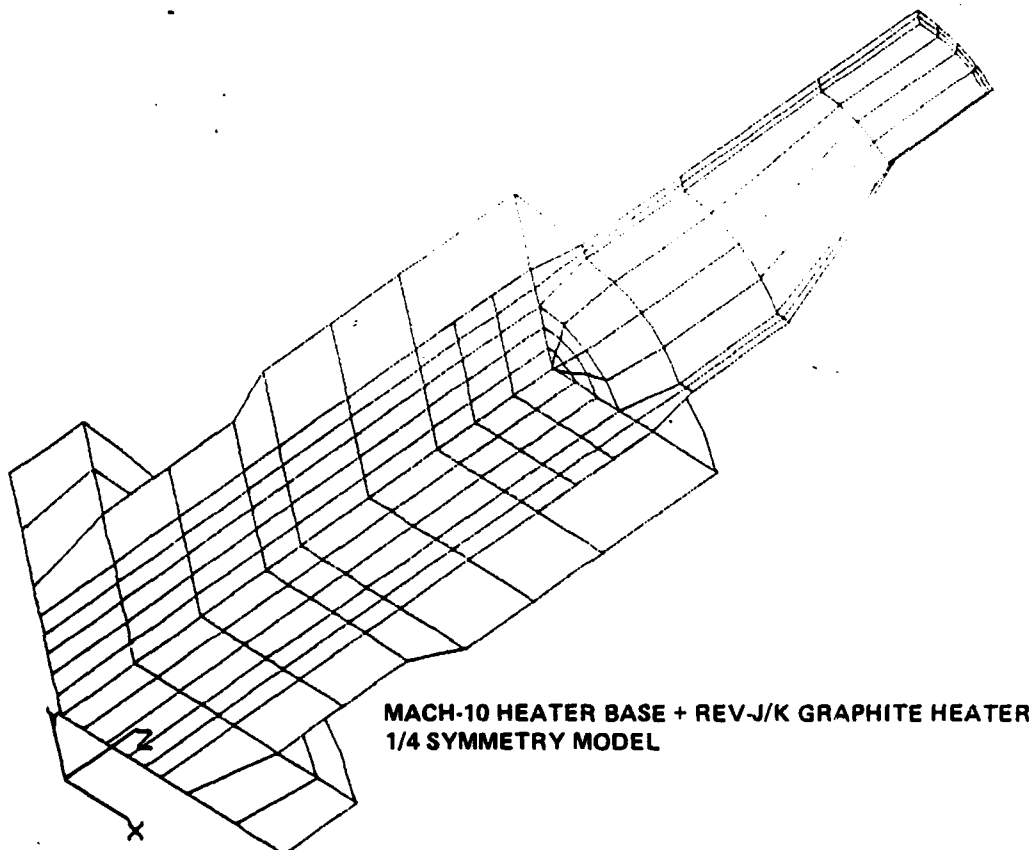
FIGURE 16. MACH-10 HEATER BASE FINITE ELEMENT MODEL

VOLTAGE POTENTIALS
TUNNEL-9 GRAPHITE HEATER
5481 AMPS , 112 VDC

56.0 =
56.0 =
56.0 =
56.0 =
55.8 =
55.7 =
55.6 = G
4.00 =
2.00 =
1.50 =
1.00 =
.750 =
.500 =
.250 = N
0. =
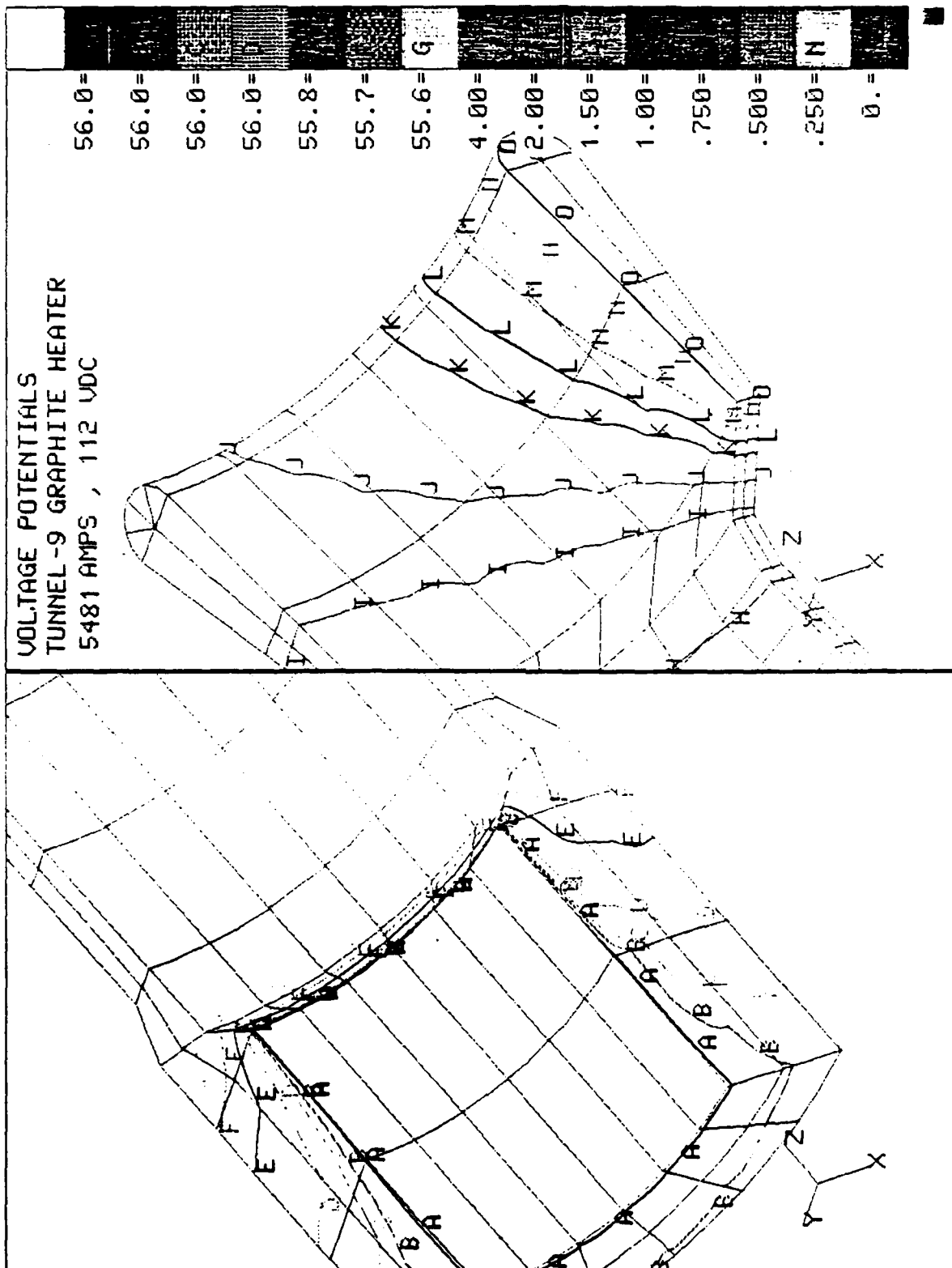
FIGURE 17. VOLTAGE POTENTIALS IN THE J HEATER

TOP   BOTTOM
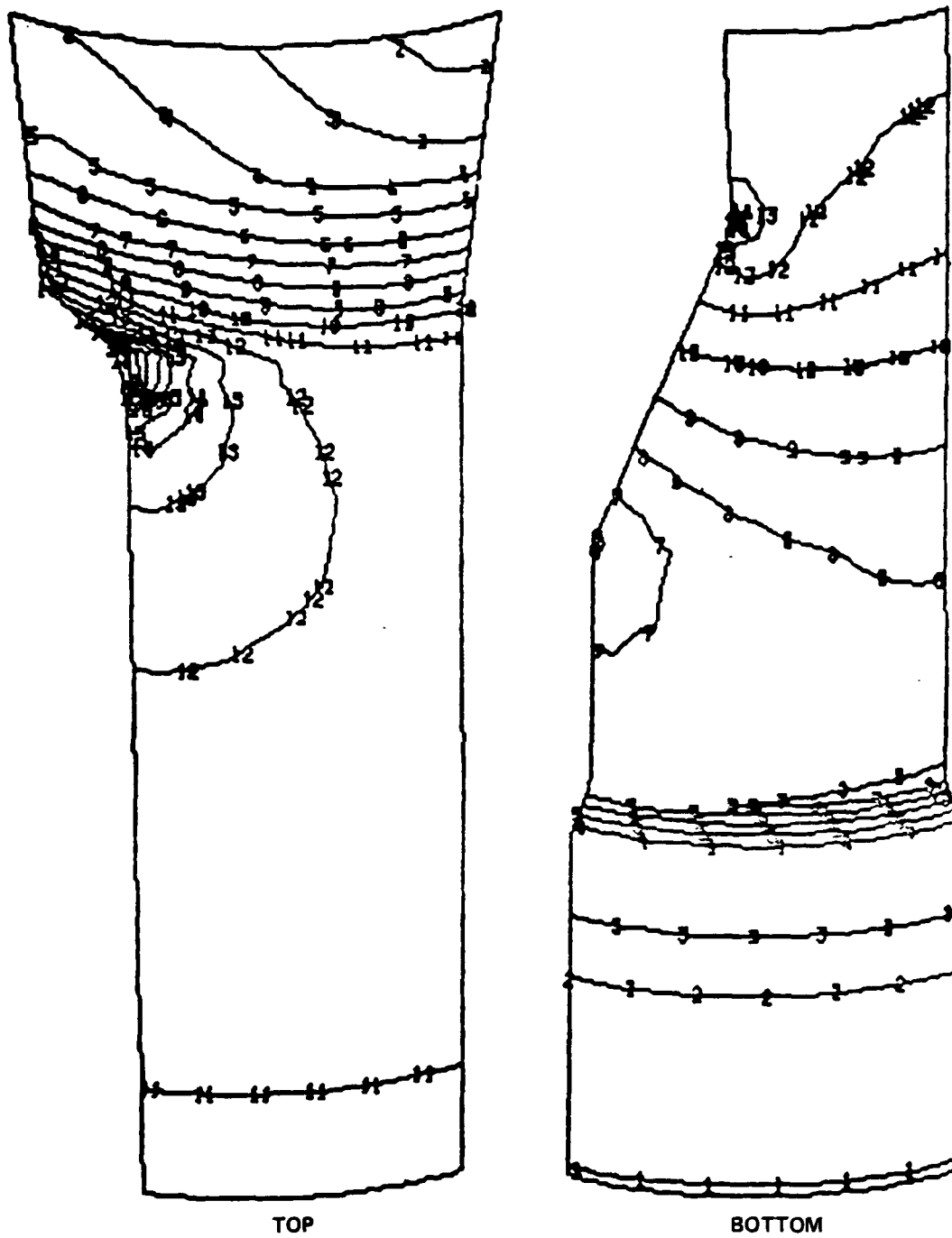
FIGURE 18. CURRENT DENSITY CONTOURS IN THE J HEATER

TEMPERATURE   F
M-14 START HEAT
STEADY STATE
N2 SINK TEMP=300F
5481 AMPS

END HEAT
CONTOUR LEVELS
USED

613.9 KW
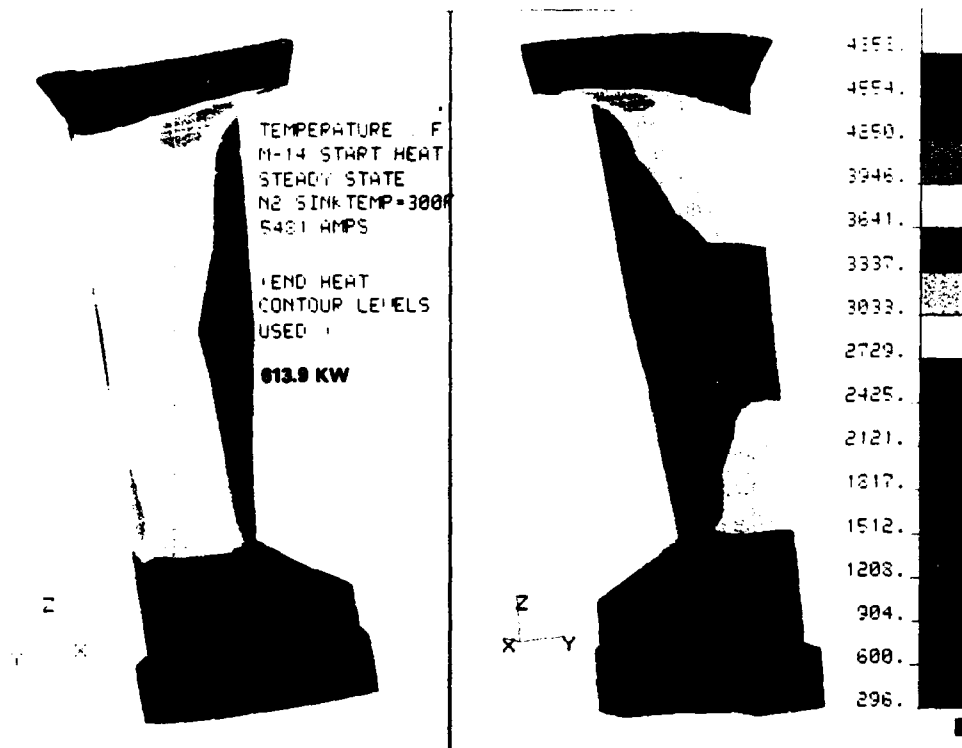
FIGURE 19. START HEAT TEMPERATURES IN THE J HEATER

TEMPERATURE , F
M-14 END HEAT
N2 TEMP=3100F
5481 AMPS

613.9 KW
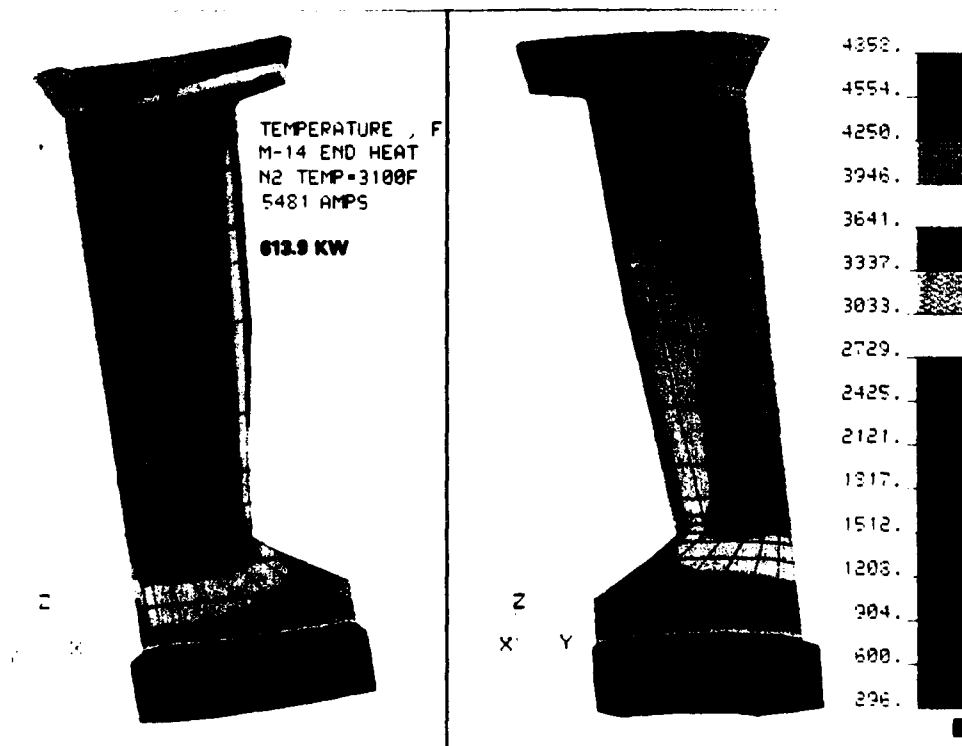
FIGURE 20. END HEAT TEMPERATURES IN THE J HEATER

TEMPERATURE F
MACH-14 END HEAT
STEADY STATE
N2 SINK TEMP= 3100F
5481 AMPS

ELEM #97-103   ELEM #241-252

4784.
4680.
4576.
4472.
4368.
4264.
4160.
4056.
3952.
3848.
3744.
3640.
3536.
3432.
3328.
3224.
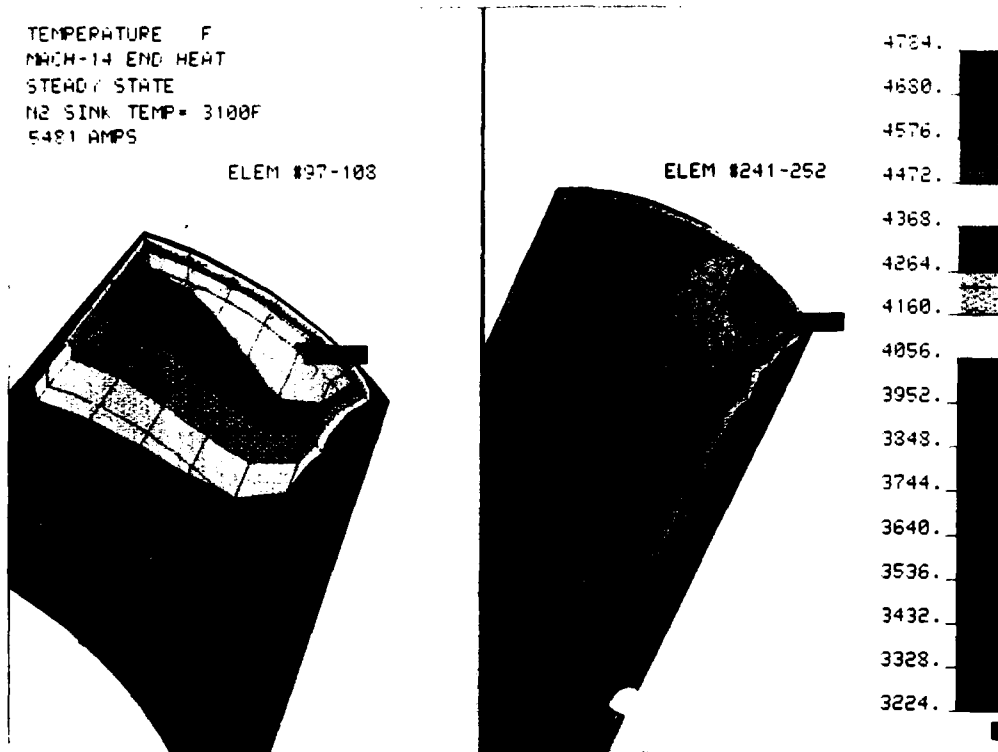
FIGURE 21. END HEAT TEMPERATURES IN THE J HEATER

TEMPERATURE, F
MACH-14 START HEAT, REV-K
GRAPHITE 5500 AMPS

3173.
3002.
2832.
2661.
2491.
2320.
2150.
1979.
1809.
1638.
1468.
1298.
1127.
957.
786.
616.

Z
X   Y
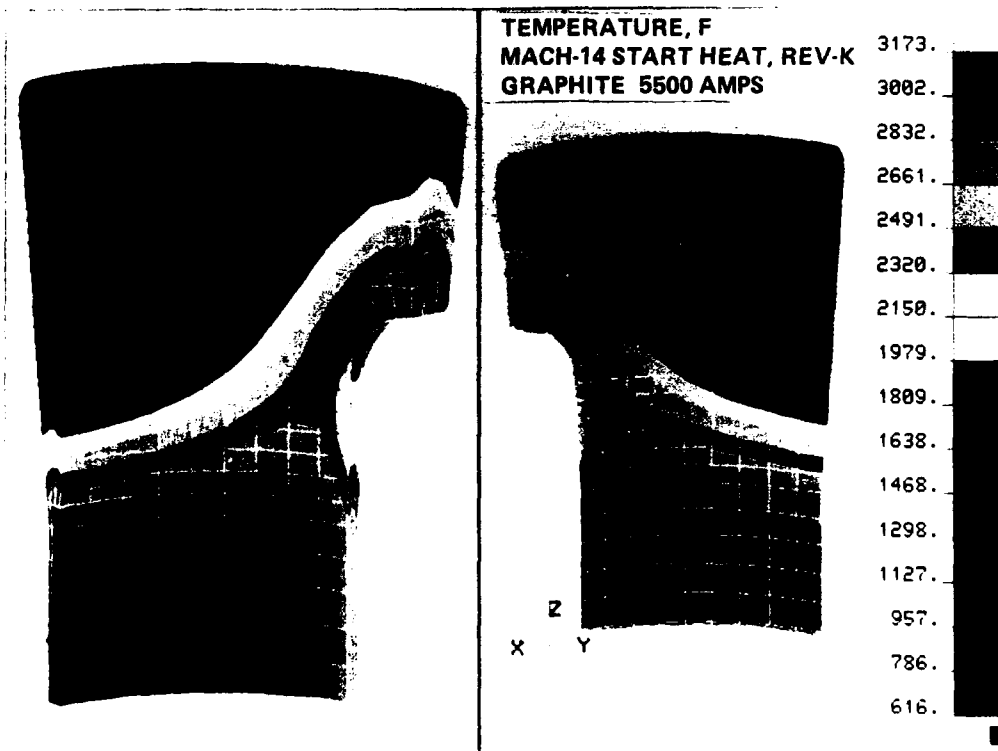
FIGURE 22. START HEAT TEMPERATURES IN THE K HEATER

TEMPERATURE F
PE'' J F GRAPHITE HEATER + MACH-10 BASE
5652 AMPS (653 KW)
N2 SINK TEMP = 500 F

| 3399. |
| 3206. |
| 3014. |
| 2821. |
| 2629. |
| 2436. |
| 2244. |
| 2051. |
| 1859. |
| 1666. |
| 1474. |
| 1281. |
| 1089. |
| 896. |
| 704. |
| 511. |
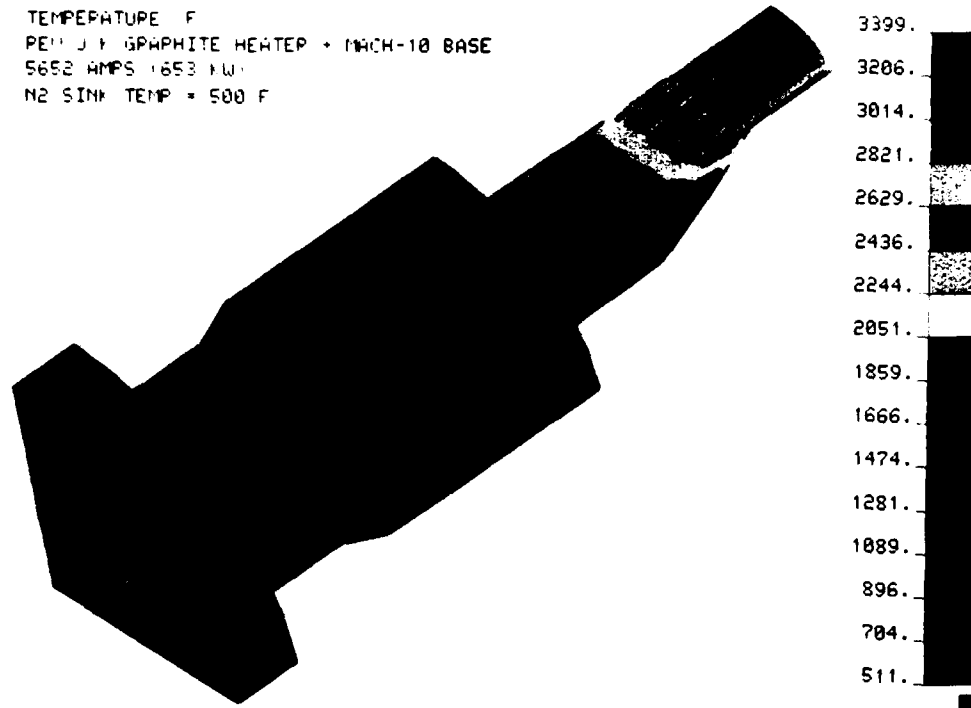
FIGURE 23. START HEAT TEMPERATURE IN THE MACH-10 BASE

ZZ-STRESS (PSI)

5652 AMPS (653 KW)
CLAMPED BASE
REV J/K GRAPHITE HEATER + MACH-10 BASE

| 5000. |
| 4500. |
| 4000. |
| 3500. |
| 3000. |
| 2500. |
| 2000. |
| 1500. |
| 1000. |
| 500. |
| 0. |
| -1000. |
| -2000. |
| -3000. |
| -4000. |
| -5000. |
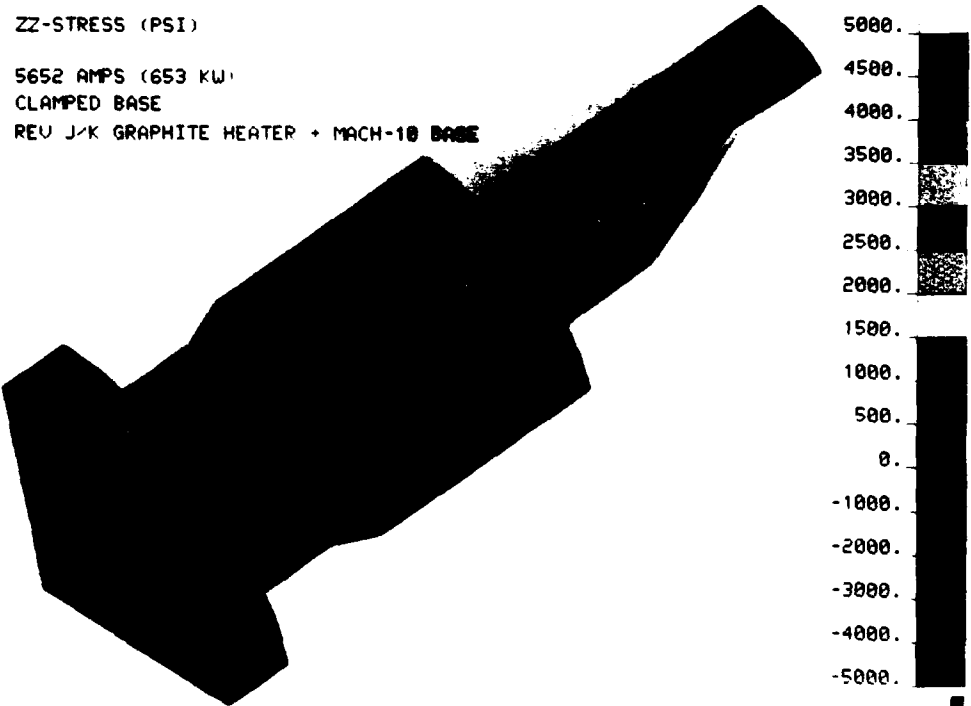
FIGURE 24. AXIAL STRESS IN MACH-10 BASE
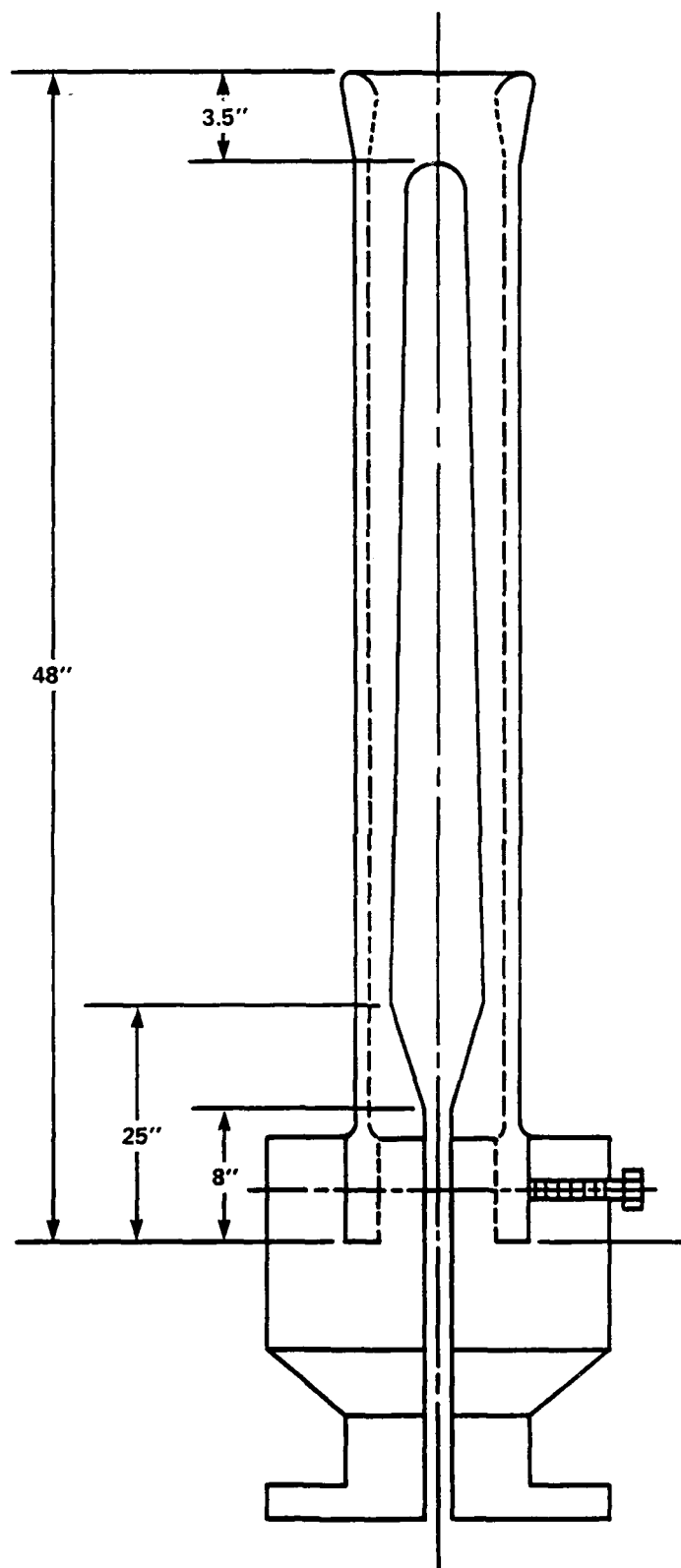
FIGURE 25. HEATER ELEMENT/BASE CLAMPING ARRANGEMENT

DEFORMATION, FREE BASE
DEF. MAGN = 4X
T-9 GRAPHITE HEATER
5481 AMPS, 112 VDC
MACH-14

START HEAT

END HEAT
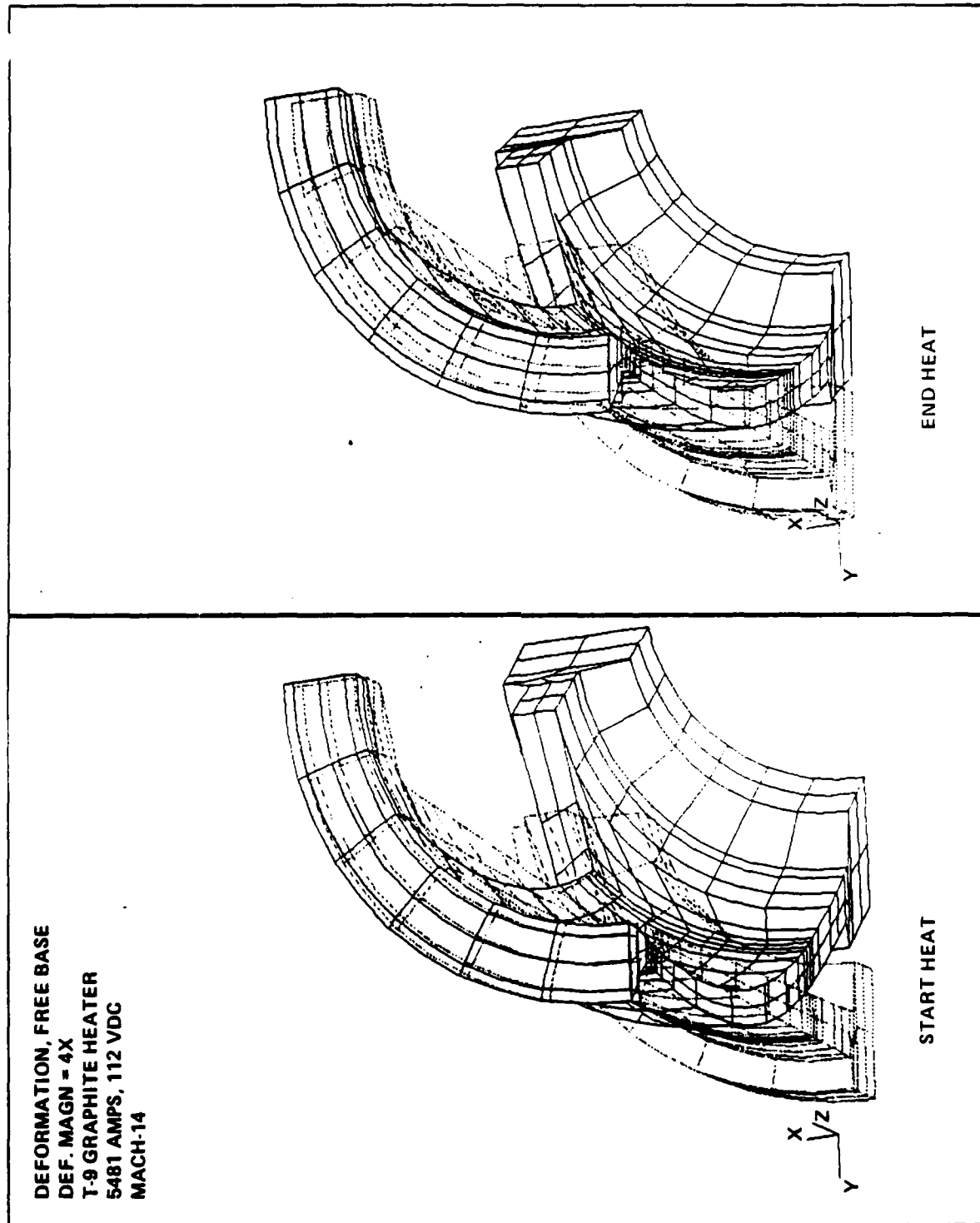
FIGURE 26. DEFORMED SHAPE PLOTS — FLOATING BASE

DEFORMATION, CLAMPED BASE
DEF. MAGN = 10X
T-9 GRAPHITE HEATER, MACH-14
5481 AMPS, 112 VDC
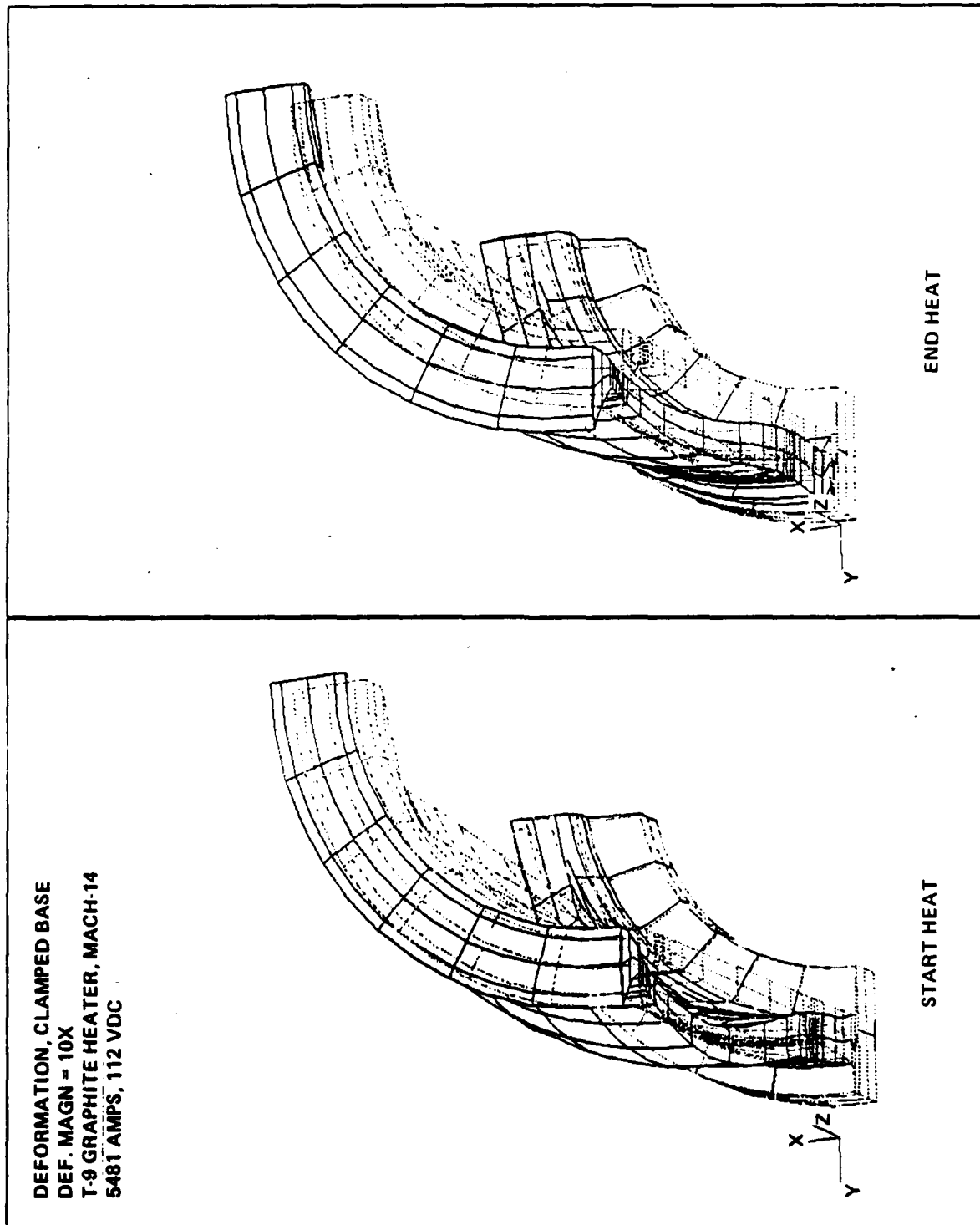
START HEAT

END HEAT

FIGURE 27. DEFORMED SHAPE PLOTS – CLAMPED BASE

ZZ STRESS (PSI)
M-14 START HEAT
CLAMPED BASE
5481 AMPS , 112V
N2 SINK=300F
GRAPHITE

INNER SURFACE

OUTER SURFACE
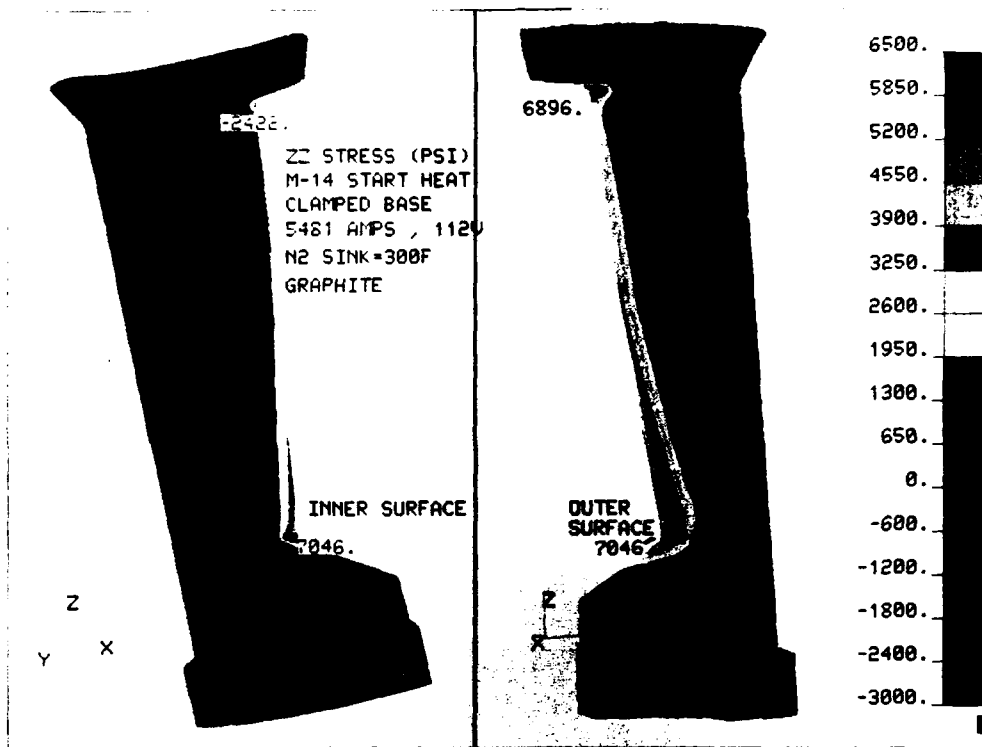
FIGURE 28. AXIAL STRESS IN J HEATER

ZZ STRESS (PSI)
REV-X GRAPHITE
5481 AMP , START HEAT
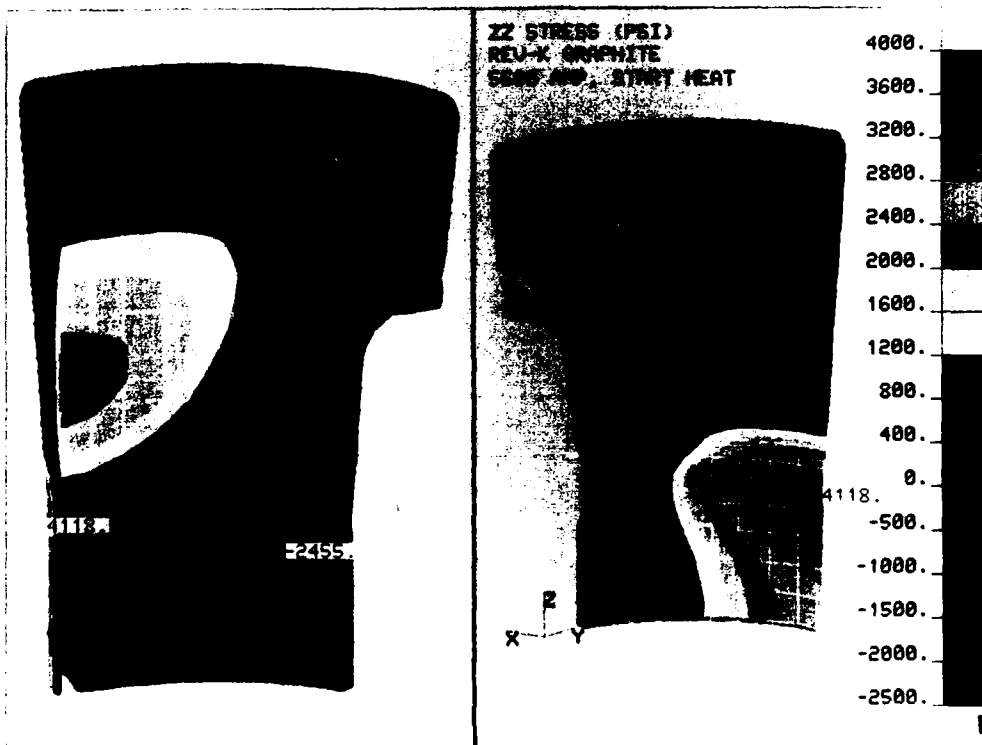
FIGURE 29. AXIAL STRESS IN K HEATER
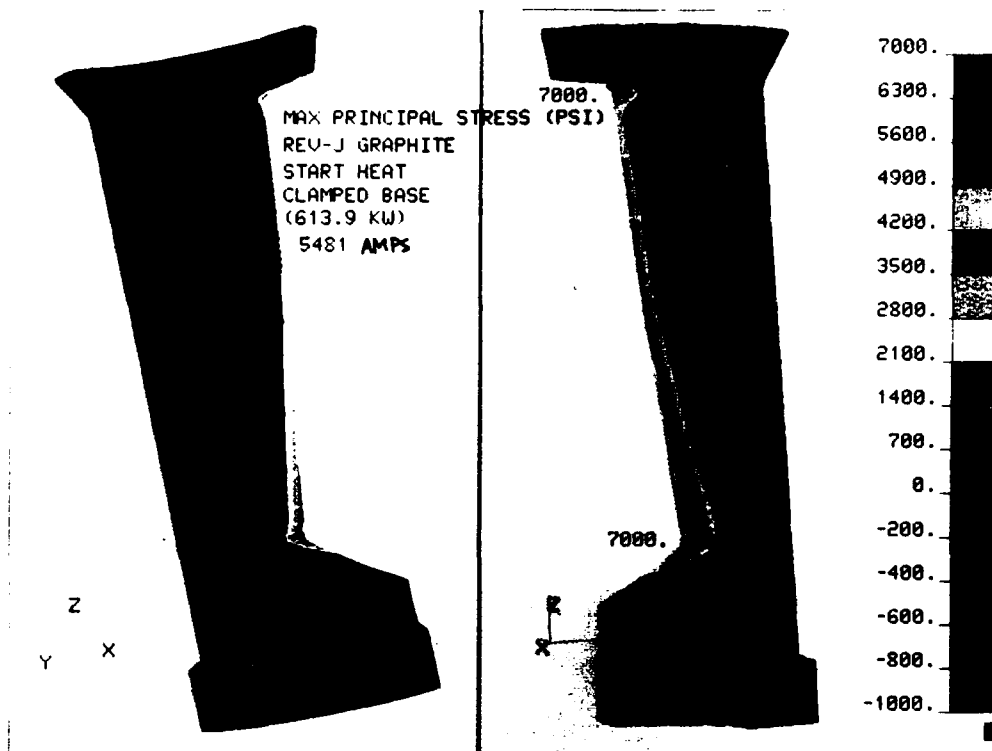
FIGURE 30. MAXIMUM PRINCIPAL STRESS — J HEATER, START HEAT
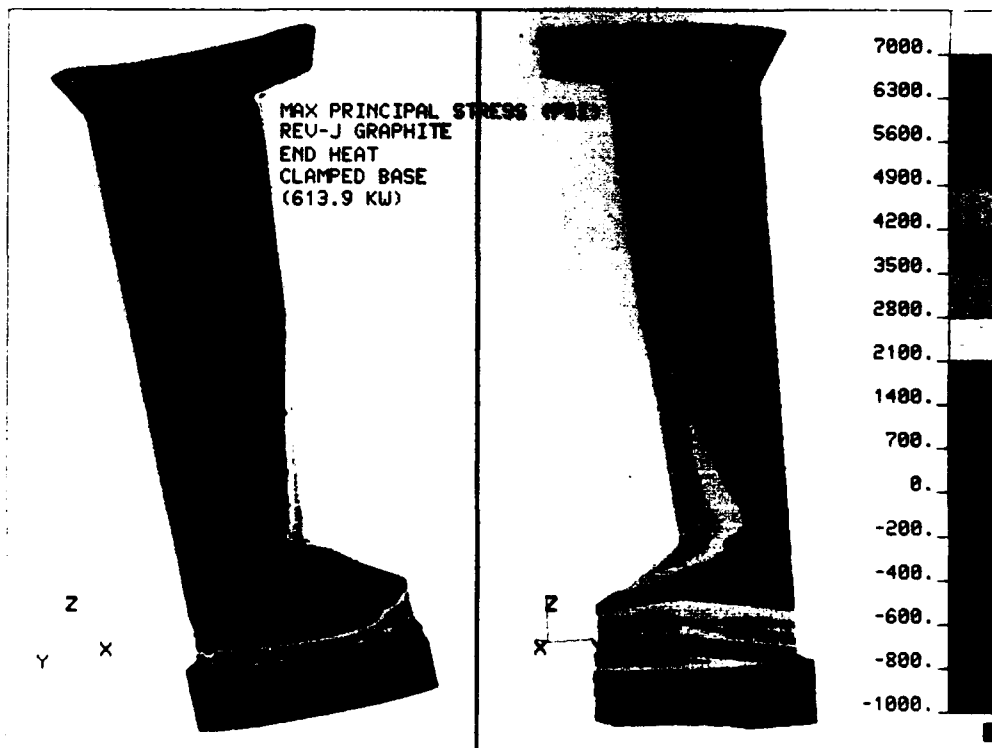
FIGURE 31. MAXIMUM PRINCIPAL STRESS — J HEATER, END HEAT
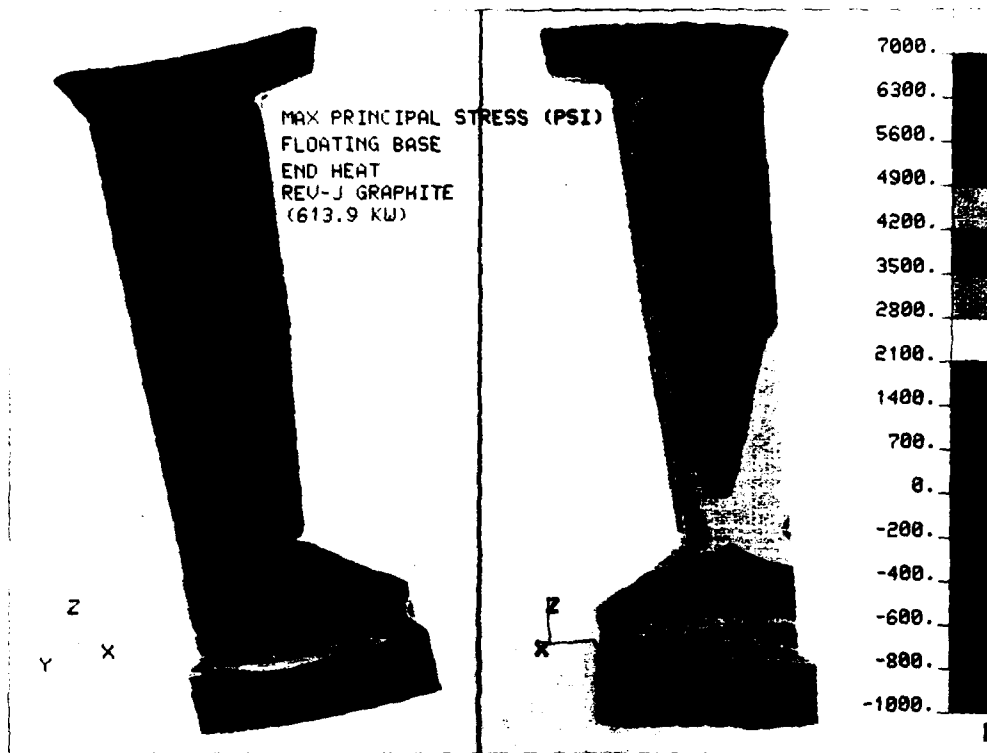
FIGURE 32. MAXIMUM PRINCIPAL STRESS – J HEATER, FREE BASE
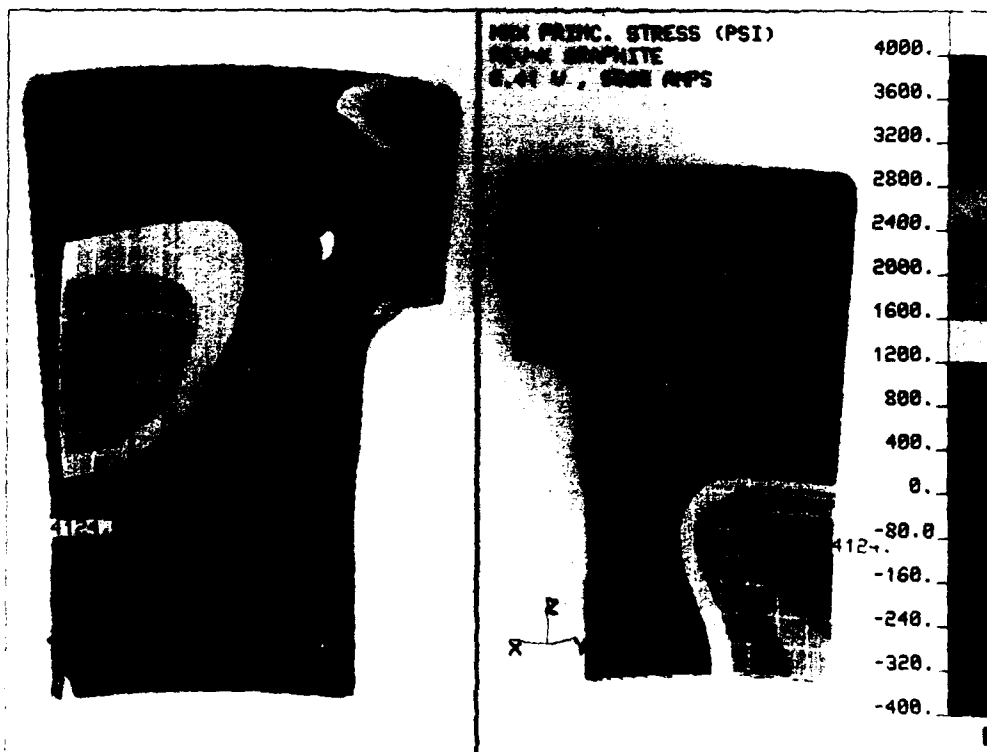
FIGURE 33. MAXIMUM PRINCIPAL STRESS – K HEATER, START HEAT
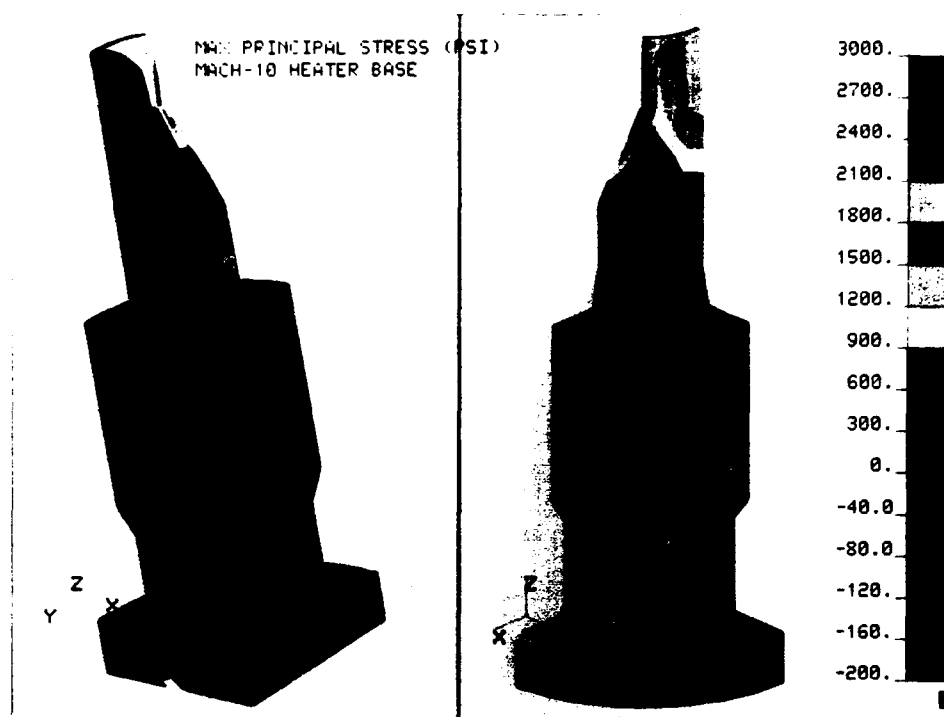
FIGURE 34. MAXIMUM PRINCIPAL STRESS — MACH-10 BASE
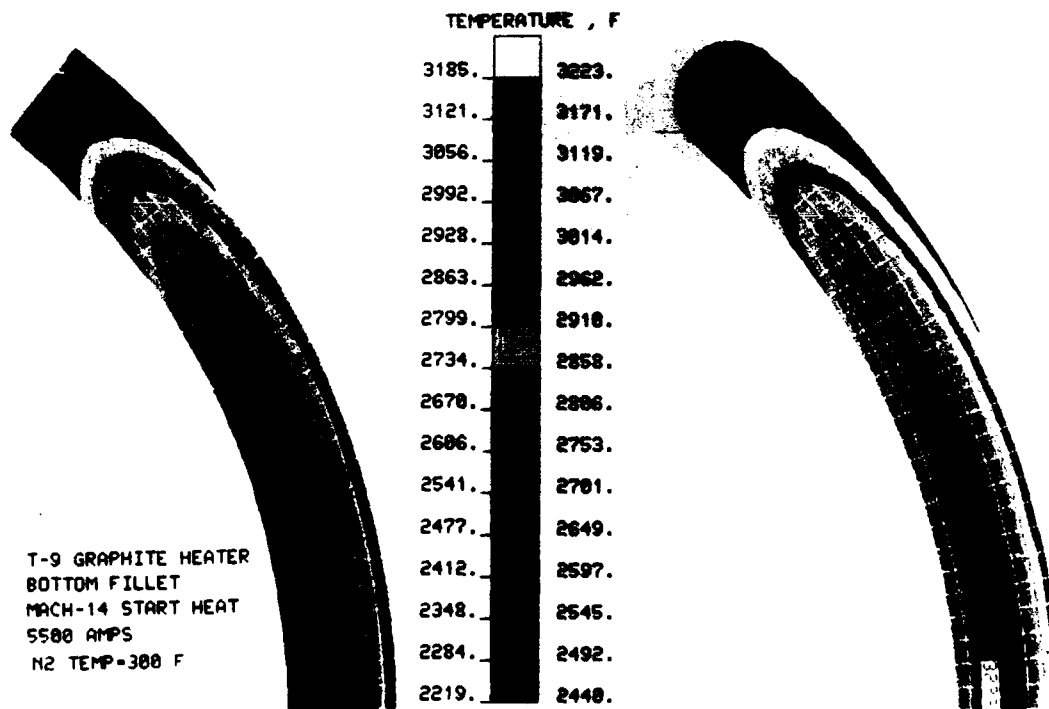
FIGURE 35. TEMPERATURE IN SQUARE AND ROUNDED CORNER HEATER LEG

49/50
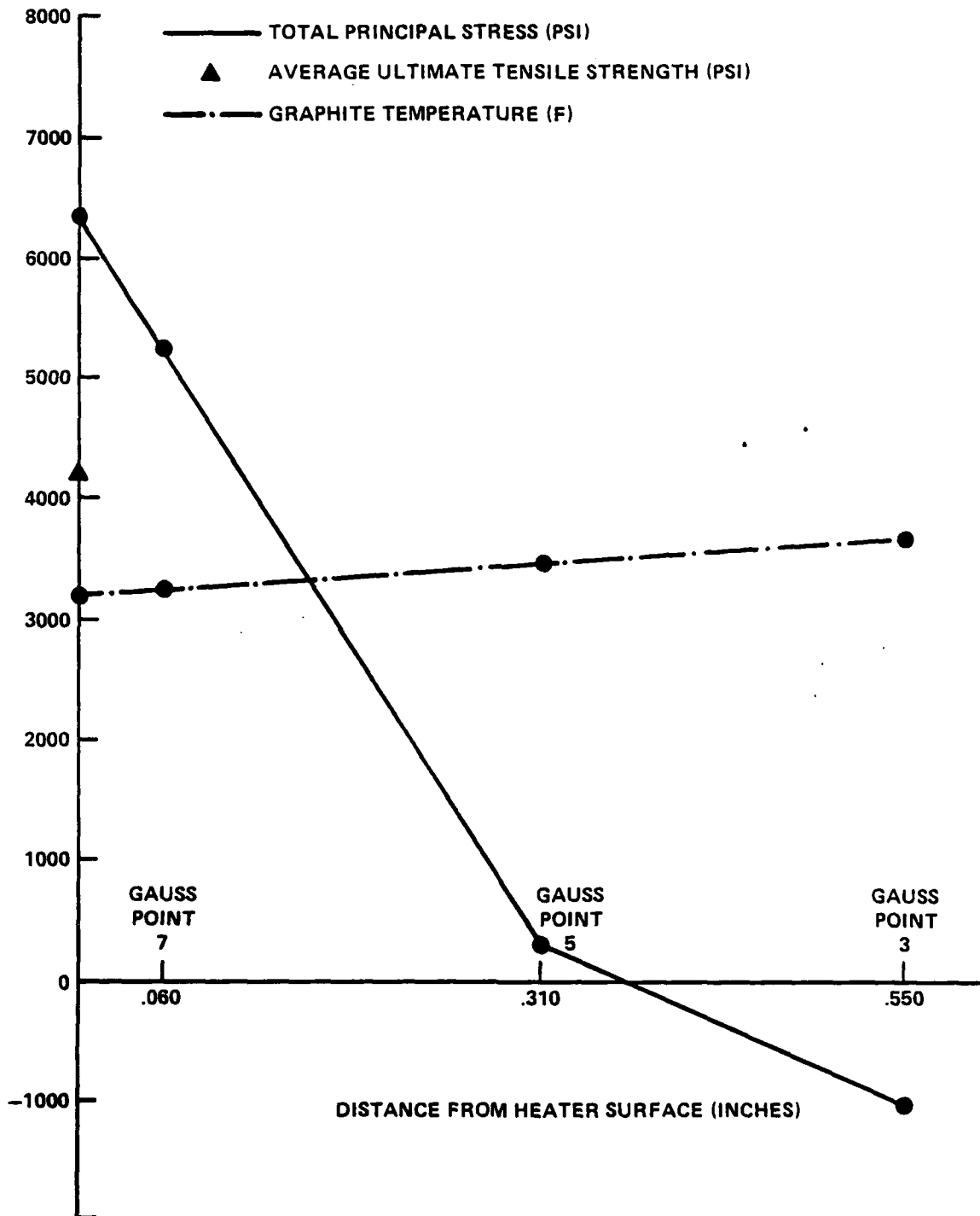
FIGURE 36. TOTAL PRINCIPAL STRESS AND TEMPERATURE PROFILES EXTRAPOLATED TO HEATER SURFACE. TOP FILLET LOCATION
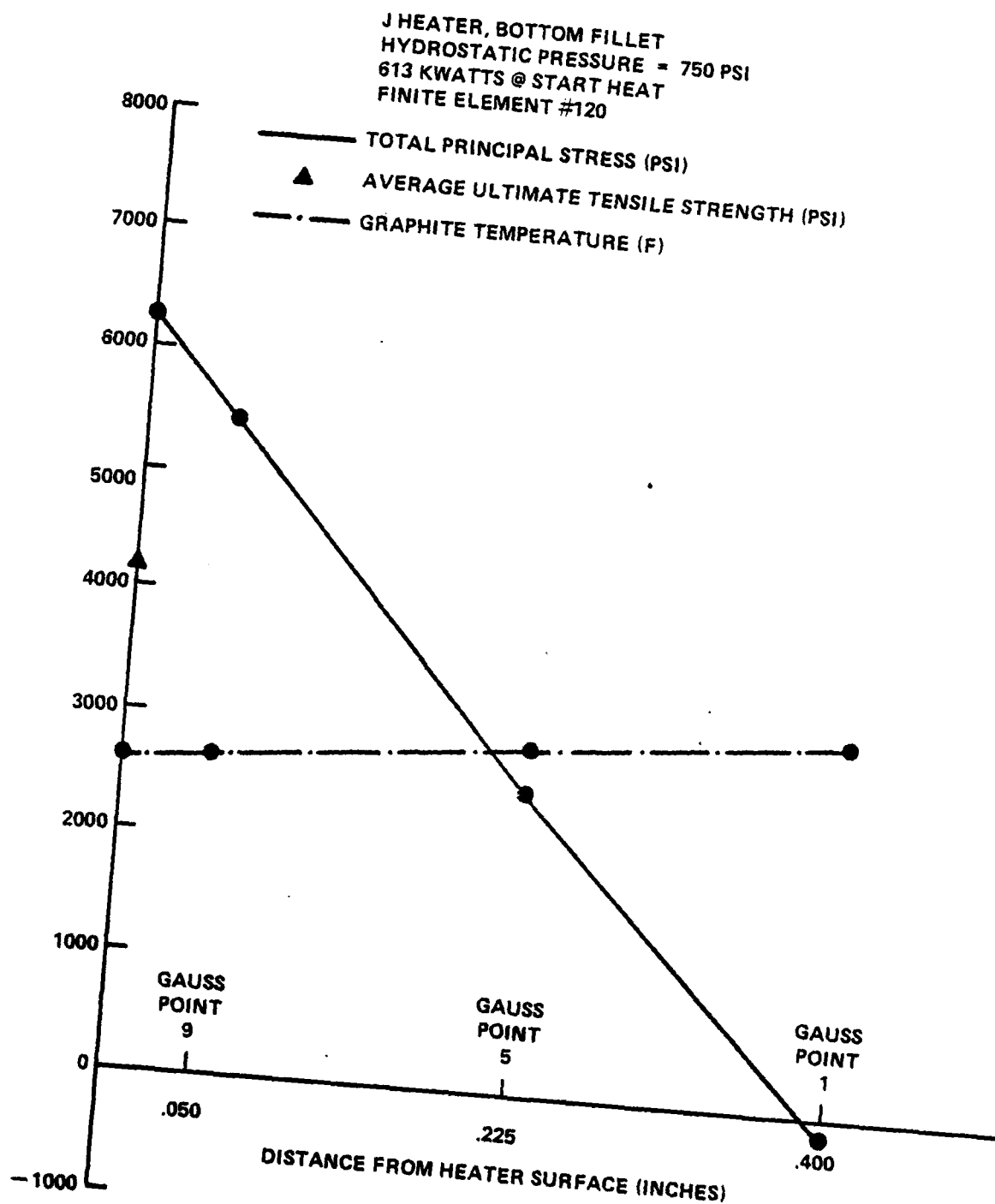
FIGURE 37. TOTAL PRINCIPAL STRESS AND TEMPERATURE PROFILES EXTRAPOLATED TO HEATER SURFACE. BOTTOM FILLET LOCATION
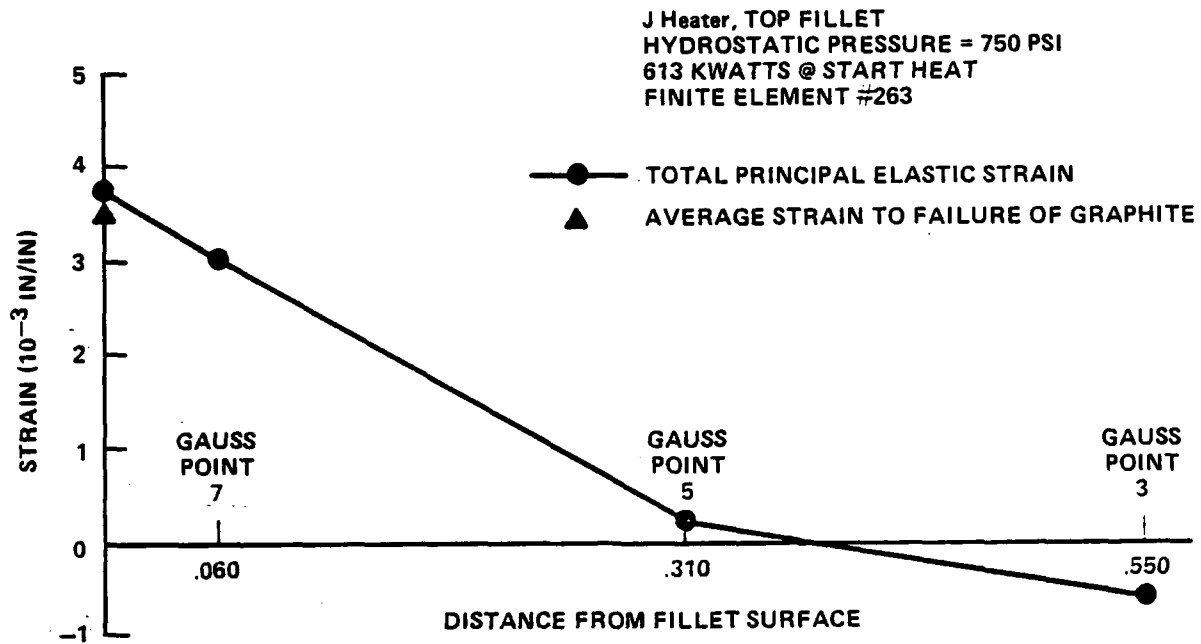
FIGURE 38. TOTAL PRINCIPAL ELASTIC STRAIN PROFILE EXTRAPOLATED TO HEATER SURFACE, TOP FILLET LOCATION
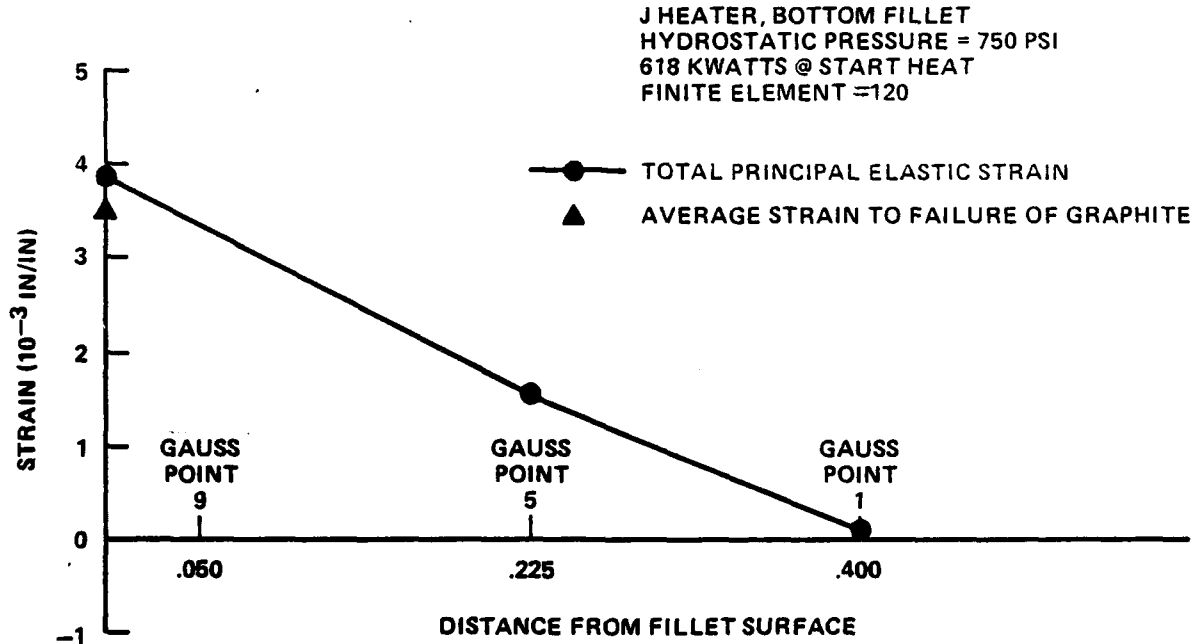
FIGURE 39. TOTAL PRINCIPAL ELASTIC STRAIN PROFILE EXTRAPOLATED TO HEATER SURFACE. BOTTOM FILLET LOCATION
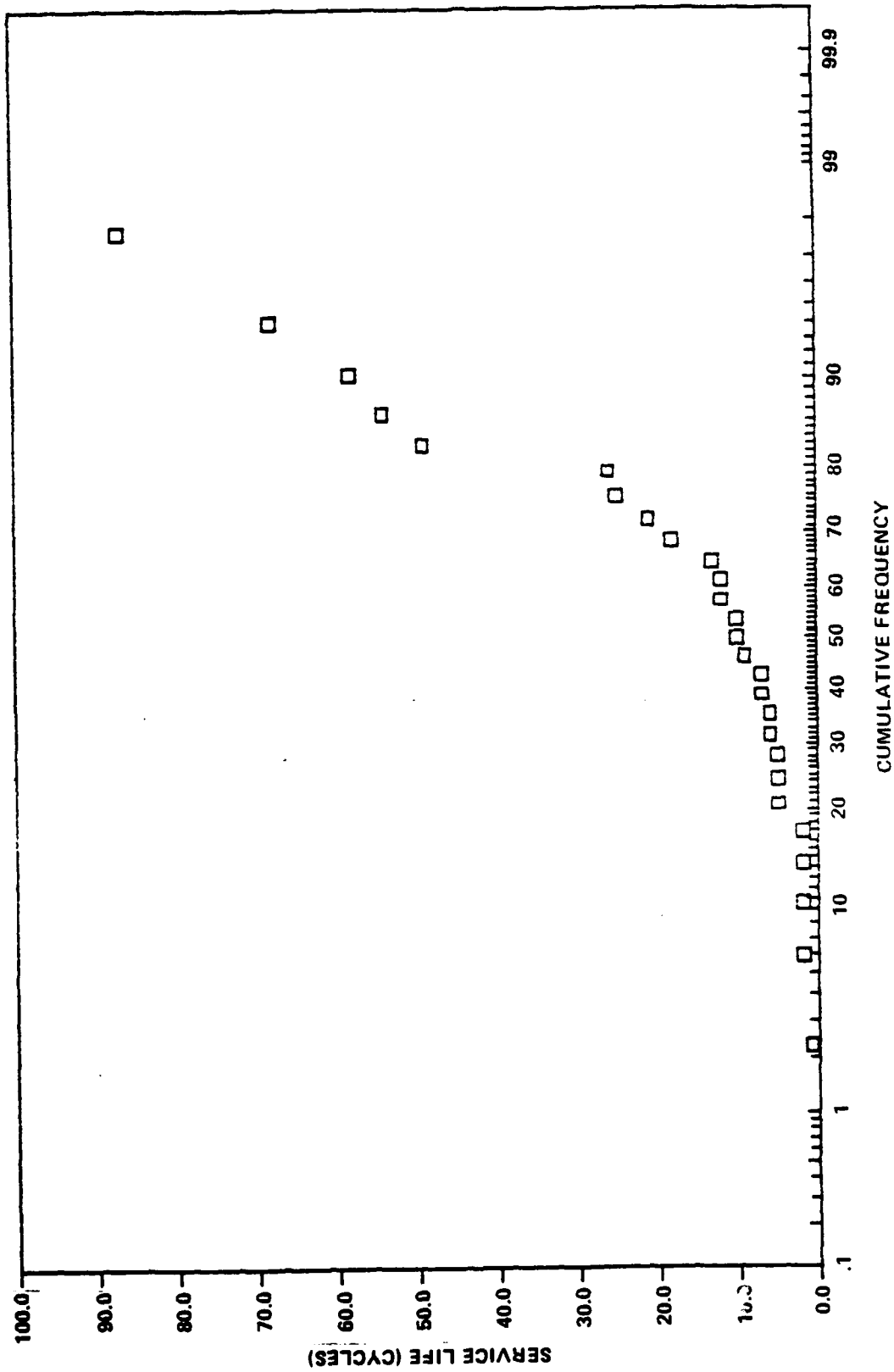
FIGURE 40.   GRAPHITE HEATER SERVICE LIFE IN TUNNEL RUNS VS. CUMULATIVE FREQUENCY
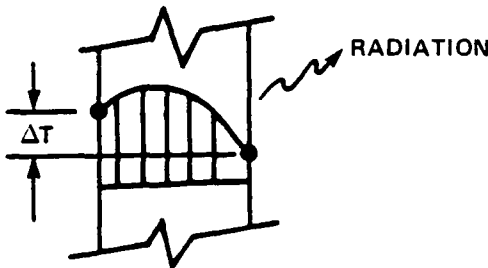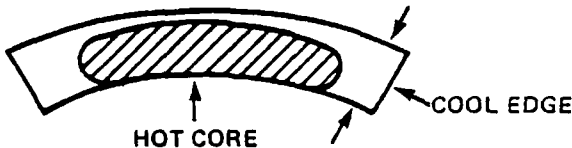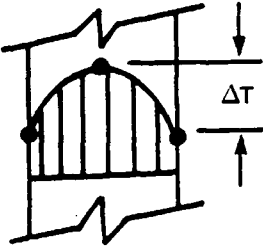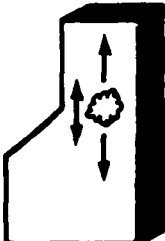
EFFECT		AMOUNT
		PSI / %

● DIFFERENTIAL RADIATION ΔT RADIATION 2917 / 42

● EDGE COOLING COOL EDGE HOT CORE 2186 / 31

● THICKNESS COOLING ΔT 1169 / 17

● BEAM BENDING (CLAMPED BASE) 437 / 6

● HOT SPOT @ FILLET 291 / 4

7000 / 100%

FIGURE 41. BREAKDOWN OF THERMAL STRESS AT BOTTOM FILLET
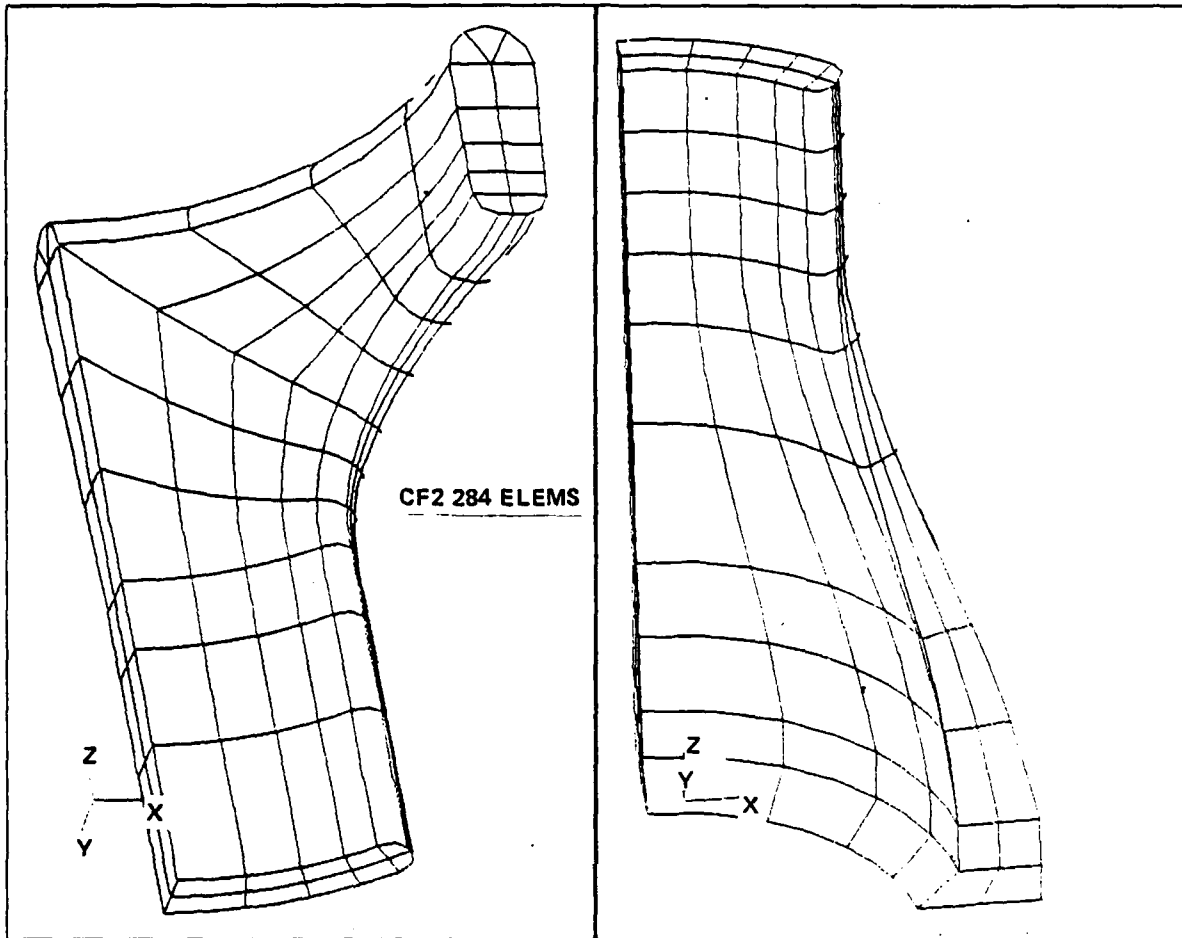
FIGURE 42.   FINITE ELEMENT MODEL WITH SLOT EDGES ROUNDED TO REDUCE FILLET STRESSES
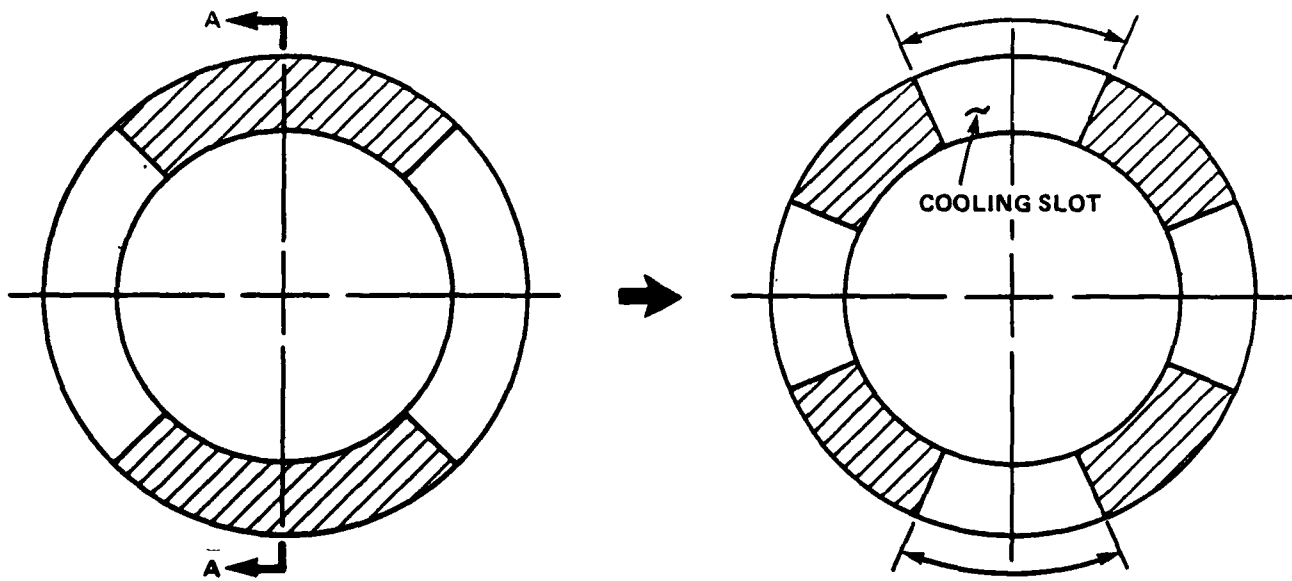
FIGURE 43.   COOLING SLOTS FORMED IN HEATER LEGS BY SECTIONING AT AA AND SEPARATING HALVES
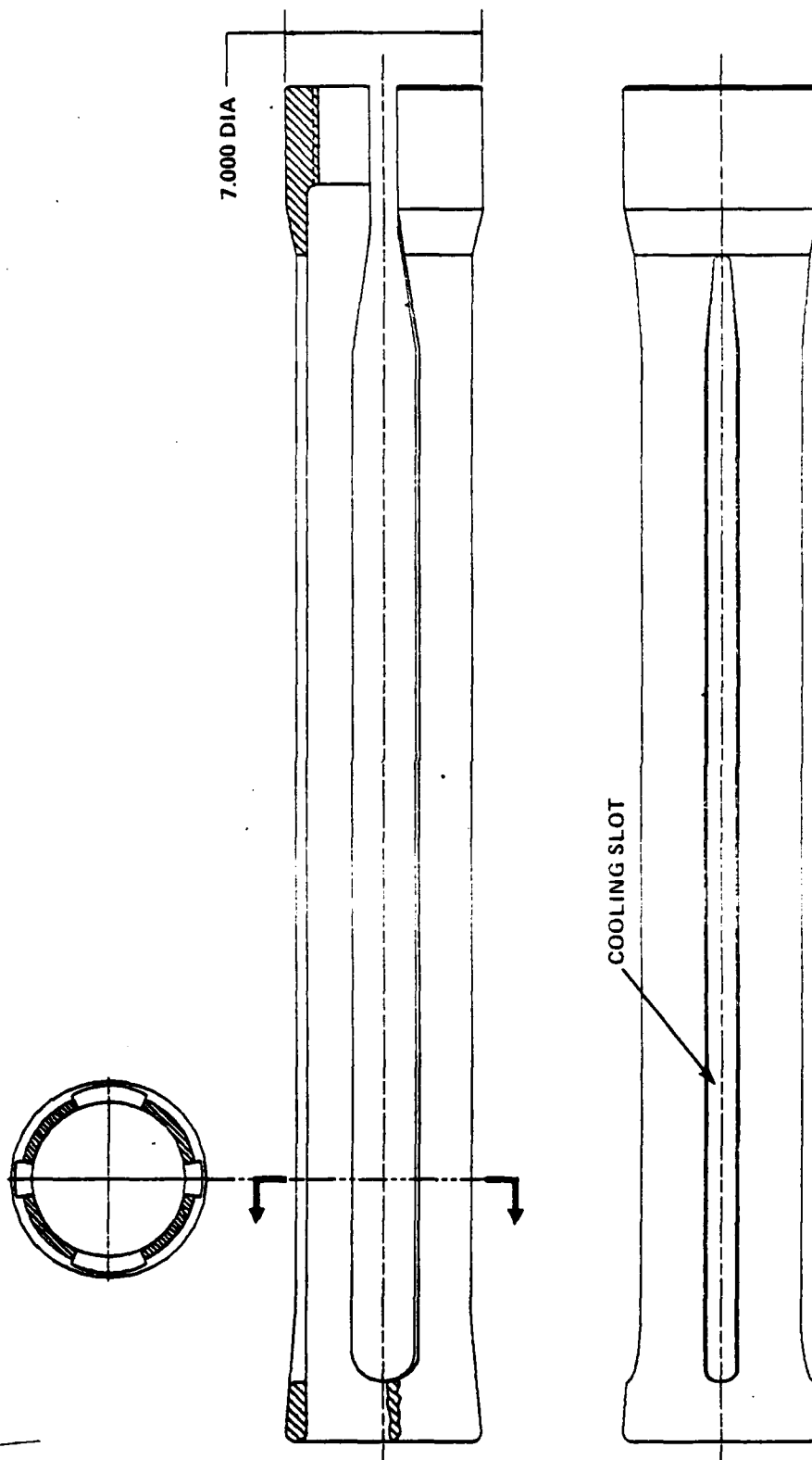
FIGURE 44. CONCEPT FOR HEATER ELEMENT WITH COOLING SLOTS

7.000 DIA

COOLING SLOT

TABLE 1. HEATER ELEMENT SERVICE LIFE HISTORY FOR 1985 AND 1986

ELEMENT LIFE
(TUNNEL RUNS)

1985 FAILURES			1986 FAILURES		
2	10	5	54	5	9
6	25	12	2	2	18
12	7	7	2	49	87
58	6	13			
1/2	10	5			
68	26	21			

↓	↓
18 ELEMENTS, 294 RUNS	9 ELEMENTS, 228 RUNS

AVERAGE RUNS PER ELEMENT = 19.3
AVERAGE ELEMENTS PER YEAR ≈ 13.5

TABLE 2. SUMMARY OF HEATER ANALYSIS STEPS

ANALYSIS STEP	ACTION	PROGRAM/INPUT	OUTPUT
1	● CREATE FINITE ELEMENT MODEL	PATRAN	2D OR 3D F.E. MODEL
	● SOLVE ELECTRICAL PROBLEM	ABAQUS	ABAQUS X. FIL RESULTS FILE
	● VERIFY CORRECT CURRENT	CURRENT/.FIL	—
	● VERIFY TOTAL HEATER POWER	POWER/.FIL	FOR054.DAT DATA FILE
	● CREATE RESISTANCE HEATING FILE	I2RFIL/.FIL	FOR032.DAT VOLUMETRIC HEATING DATA FILE
2	● SOLVE FOR TEMPERATURES IN HEATER	ABAQUS/FOR032.DAT/ DFLUX. FOR	ABAQUS.FIL FILE CONTAINING TEMPERATURES
3	● SOLVE FOR THERMAL STRESSES IN HEATER	ABAQUS/.FIL FILE FROM STEP 2	ABAQUS.FIL FILE CONTAINING THERMAL STRESS/STRAIN

59

TABLE 3. HEAT TRANSFER INPUT DATA

		RADIATION/CONVECTION SINK TEMPS		PRESCRIBED TEMP	MACH 14			
					START HEAT		END HEAT	
CONFIG.	REGION	START HEAT	END HEAT		$\bar{h}$	EMISSIVITY	$\bar{h}$	EMISSIVITY
		R/C	R/C	°F	BTU/FT²·HR·R		BTU/FT²·HR·R	
J/K	WETTED O.D.	300/300	3100/3100	–	88.5	.85	117	.85
J/K	WETTED I.D.	–/300	–/3100	–	88.5	–	117	–
J/K	WETTED SLOT EDGES	300/300	3100/3100	–	88.5	.85	117	.85
J/K	RADIUS CROWN	300/300	3100/3100	–	88.5	.85	117	.85
J	THREADED BASE OD & ID	–/–	–/–	300*	:	–	–	–
BASE	WETTED O.D.	500/500	–	–	100.0	.85	–	–
	WETTED TOP SURFACE	500/500	–	–	100.0	.86	–	–
	WETTED BOTTOM SURFACE	500/500	–	–	80.0	.85	–	–
	WETTED FLAT	–/500	–	–	100.0	.85	–	–
	THREADED HEATER BASE:							
	– OD SURFACE	–/500	–	–	25.0	–	–	–
	– MATCHING BASE SURFACE	–/500	–	–	25.0	–	–	–
	THREADED HEATER BASE:							
	– BOTTOM SURFACE	/500	–	–	25.0	–	–	–
	– MATCHING BASE SURFACE	/500	–	–	25.0	–	–	–
	J/K HEATER OD	500/500	–	–	100.0	.85	–	–
	J/K HEATER ID	/500	–	–	100.0	–	–	–
	J/K HEATER SLOT EDGE	500/500	–	–	100.0	.85	–	–

*FOR 913 KWATT CASE THESE SURFACES TREATED SAME AS WETTED O.D. & I.D. OF HEATER LEGS.

TABLE 4. PEAK THERMAL STRESS-STRAIN STATES IN GRAPHITE HEATER

FILLET	ELEM/GS. PT.	HEAT PERIOD	STRESS/TOTAL STRAIN/ELASTIC STRAIN COMPONENTS (PSI) (IN/IN) (IN/IN)						MAX PRINCIPAL		TEMP (F)
			XX	YY	ZZ	XY	XZ	YZ	STRESS (PSI)	TILT ANGLE (FROM ZZ) (DEGREES)	
TOP	263/7	START	-152	642	5471	-192	385	-1273	5815	14.5	3221
			1.024E-02	1.077E-02	1.399E-02	-2.559E-04	5.138E-04	-1.699E-03			
			-6.591E-04	-2.932E-05	3.193E-03	-2.559E-04	5.138E-04	-1.699E-03			
BOTTOM	120/9	START	319	168	6021	-194	-244	592	6092	6.3	2669
			8.455E-03	8.351E-03	1.239E-02	-2.672E-04	-3.36E-04	8.165E-04			
			-2.964E-04	-4.001E-04	3.634E-03	-2.672E-04	-3.36E-04	8.165E-04			
TOP	263/7	END	-118	827	5317	-250	397	-1684	5913	9.0	4192
			1.403E-02	1.465E-02	1.763E-02	-3.320E-04	5.26E-04	-2.232E-03			
			-5.375E-04	8.886E-05	3.064E-03	-3.320E-04	5.26E-04	-2.232E-03			
BOTTOM	119/7	END	44.8	478	6169	-215	-384	793	6304	8.8	3829
			1.265E-02	1.293E-02	1.667E-02	-2.828E-04	-5.037E-04	1.041E-03			
			-4.760E-04	-1.918E-04	3.545E-03	-2.828E-04	-5.037E-04	1.041E-03			

TABLE 5. PROBABILITY OF FAILURE FOR GRAPHITE HEATERS

HEATER CONFIG.	HEATER POWER (KWATTS)	HEATING PERIOD	FILLET LOCATION	PRINCIPAL STRESS STRAIN	HYDRO-STATIC STRESS STRAIN	TOTAL PRINCIPAL STRESS STRAIN	P.O.F. %
J	613	START	TOP	7000 PSI	750	6250	100
			TOP	.00407 IN/IN	.000326	.00375	65
J/K	613	START	BOTTOM	7000 PSI	750	6250	100
			BOTTOM	.00419 IN/IN	.000326	.00387	75
J*	913	START	TOP	8615 PSI	750	7865	100
			TOP	.00500 IN/IN	.000326	.00468	100

*ESTIMATED DATA BASED ON A SIMILAR END HEAT ANALYSIS

REFERENCES

1. Southern Research Institute, <u>Evaluation and Comparison of</u>
    <u>Graphite Heater Tube Materials Used in the Hypervelocity</u>
    <u>Wind Tunnel</u>, SoRI-EAS-86-508-5787-I-F, Southern Research
    Institute, Birmingham, AL, Jul 1986.

2. <u>ABAQUS</u> (Version 4-5), Hibbitt, Karlsson, and Sorensen, Inc.,
    Providence, RI, Jul 1985.

3. <u>PATRAN</u>, PDA Engineering, Santa Ana, CA, Dec 1985.

4. Schneider, P. J., <u>Conduction Heat Transfer</u>, Addison-Wesley
    Publishing Company, Inc., Reading Massachusetts, pp 338,
    1955.

5. Juvinall, R. C., <u>Stress, Strain, and Strength</u>, McGraw-Hill
    Book Co., Inc., New York, NY, 1967.

6. Dieter, G. E., <u>Mechanical Metallurgy</u>, Second Edition,
    McGraw-Hill Book Co., Inc., NewYork, NY, 1976.

7. Buch, J. D., Crose, J. G., and Robinson, E. Y., <u>Failure</u>
    <u>Criteria in Graphite Program</u>, AFML-TR-77-16, Air Force
    Materials Laboratory, Wright Patterson Airforce Base, OH,
    Mar 1977.

APPENDIX   A

ANALYSES SUPPORT PROGRAMS

```
      PROGRAM CURRENT

C     PROGRAM TO COMPUTE TOTAL CURRENT IN ABAQUS
C     HEATER MODEL BY SUMMING REACTION FLUXES FROM
C     ABAQUS THERMAL ANALYSIS RESULTS. USER MUST SUPPLY
C     NODES IN THE DATA STATEMENT WHICH DEFINE CROSS-
C     SECTION FOR WHICH TOTAL CURRENT IS DESIRED.
C     USER MUST UPDATE NODEN AND IMPLIED DO LIMIT BELOW.
C     BEFORE RUNNING ASSIGN THE XXX.FIL FILE
C     TO FORTRAN UNIT FOR008. ONLY NODES FOR WHICH TEMPERATURES
C     HAVE BEEN PRESCRIBED CAN BE SPECIFIED.

      IMPLICIT REAL*8(A-H,O-Z)
      DOUBLE PRECISION ARRAY
      DIMENSION ARRAY(513), JRRAY(2,513) , NSET(500)
      EQUIVALENCE (ARRAY(1) , JRRAY(1,1))
      CALL INITF

      NODEN=29
      RFLUX=0.0
C
      DATA (NSET(L),L=1,29) /
     1 109,   110,   111,   112,   113,   114,
     2 115,   116,   117,   118,   119,   120,
     3 382,   383,   384,   385,
     4 386,   387,   388,   389,   390,   391,
     5 392,   393,   394,   395,   396,   397,   398/

C
      K=1
      DO WHILE (K.LE.999999)
         CALL DBFILE (0,ARRAY,JRCD)
         IF (JRCD.NE.0) GO TO 100
         KEY= JRRAY(1,2)
         IF (KEY.EQ.214) THEN
            M=1
            DO WHILE (M.LE.NODEN)
               IF (NSET(M).EQ.JRRAY(1,3)) THEN
                  RFLUX=RFLUX+ARRAY(4)
               END IF
            M=M+1
            END DO
         END IF
      K=K+1
      END DO
  100 CURENT= RFLUX*2.0
      WRITE (6,2000) CURENT
 2000 FORMAT(10X,24H TOTAL HEATER CURRENT = F10.3,1X,7HAMPERES)
      STOP
      END
```

```
      PROGRAM I2RFIL

C     PROGRAM TO READ FLUXES AT MAT'L CALCULATION
C     POINTS (=GAUSS PTS FOR DC3D20) FROM ABAQUS
C     GENERATED XXX.FIL FILE AND CONVERT FLUXES TO
C     ELECTRICAL RESISTANCE (I2R) HEATING VALUES. PROGRAM
C     WRITES HEATING VALUES TO FILE UNIT 032. BEFORE
C     RUNNING ASSIGN THE XXX.FIL FILE TO FORTRAN UNIT
C     FOR008. PROGRAM ASSUMES FLUXES ARE CURRENT
C     DENSITIES.

      IMPLICIT REAL*8(A-H,O-Z)
      DOUBLE PRECISION ARRAY
      DIMENSION ARRAY(513), JRRAY(2,513)
      EQUIVALENCE (ARRAY(1) , JRRAY(1,1))
      CALL INITF

C***** SPECIFY MATERIAL ELECTRICAL CONDUCTIVITY, SIGMA
C***** FOR BODY FLUX UNITS OF BTU/SEC-CU.IN.
C***** USE SIGMA UNITS OF (OHM-IN)**-1
C
      SIGMA=2032.0

      DO 100 K = 1 , 99999
        CALL DBFILE(0,ARRAY,JRCD)
      IF(JRCD.NE.0) GO TO 110
      KEY=JRRAY(1,2)
      IF(KEY.EQ.1) GO TO 10
      IF(KEY.EQ.28) GO TO 20
      GO TO 100
   10 CONTINUE
      JEL=JRRAY(1,3)
      JPNT=JRRAY(1,4)
      GO TO 100
   20 CONTINUE
      RBFLUX=ARRAY(3)*ARRAY(3)/SIGMA
C
C***** CONVERSION FOR BODY FLUX UNITS OF B.T.U./SEC-CU.IN.
      RBFLUX=RBFLUX*0.000948451

      WRITE(32,120)  JEL,JPNT,RBFLUX
  120 FORMAT(2I5,E10.3)
  100 CONTINUE
  110 CONTINUE
      ENDFILE 32
      STOP
      END
```

```
      SUBROUTINE DFLUX (FLUX,TEMP,KSTEP,KINC,TIME,NOEL,NPT,COORDS,JLTYP)
      IMPLICIT DOUBLE PRECISION (A-H,O-Z)
      DIMENSION COORDS(3), RBFLUX(1000,27)
      DATA KSET/0/
C*****
C***** FLUXES ARE READ FROM FILE 32 AND LOADED
C***** INTO LOOK-UP TABLE RBFLUX ON FIRST CALL
C***** OF THIS SUBROUTINE
C*****
      IF (KSET.EQ.0) THEN
          DO 20 I=1,30000
              READ(32,1000,END=30) NNOEL,NNPT,BFLUX
 1000         FORMAT(2I5,E10.3)
              RBFLUX(NNOEL,NNPT)=BFLUX
 20       CONTINUE
 30   KSET=1
      END IF
C*****
C***** DEFINE FLUX
C*****
      FLUX=RBFLUX(NOEL,NPT)
      RETURN
      END
```

```
      PROGRAM POWER
*  TO RUN THIS PROGRAM YOU MUST:
*           (1) ASSIGN A XXX.FIL FILE TO A FORTRAN FOR008 FILE
*           (2) LINK/NOMAP/EXE:POWER POWER,VAXA$DUA1:[ABAQUS]ABQ5LIB/LIB
*
*   THIS PROGRAM WILL COMPUTE:
*
*   THE TOTAL POWER GENERATED IN THE MODEL, TOTAL VOLUME OF THE MODEL
*    AND IT WILL SHOW THE AVERAGE POWER GENERATED FROM EACH ELEMENT
*
*      THE ELEMENTS MAKE UP ONE QUARTER OF THE MODEL, SO
*      THE TOTAL VOLUME AND TOTAL POWER IS MULTIPLIED BY 4 IN PROGRAM
*


      IMPLICIT REAL*8(A-H,O-Z)
      DOUBLE PRECISION ARRAY
      DIMENSION ARRAY(513),JRRAY(2,513)


*
* YOU MAY WANT TO CHANGE THE VALUES DIMENSIONED IF YOU HAVE A
*        LARGER OR SMALLER MODEL

      DIMENSION NODE(5000), X(5000), Y(5000), Z(5000)
      DIMENSION NELE(1000),NOD1(1000),NOD2(1000),NOD3(1000),NOD4(1000)
      DIMENSION NOD5(1000), NOD6(1000), NOD7(1000), NOD8(1000)
      DIMENSION AVE(1000), NELA(1000), VOL(1000)

      EQUIVALENCE (ARRAY(1) , JRRAY(1,1))
      CALL INITF

      L=0
      N=0
      DO 500 K = 1,99999
          CALL DBFILE(0,ARRAY,JRCD)
            IF (JRCD.NE.0) GO TO 500
             KEY = JRRAY(1,2)

*
* KEY 1901 IS USED TO OBTAIN THE COORDINATES OF EACH NODE
*

              IF(KEY.EQ.1901) THEN
                N=N+1
                NODE(N) = JRRAY(1,3)
                X(N) = ARRAY(4)
                Y(N) = ARRAY(5)
                Z(N) = ARRAY(6)

*
* KEY 1900 IS USED TO OBTAIN THE NODE POINTS OF EACH ELEMENT
*
```

```
        ELSE IF (KEY.EQ.1900) THEN
            L=L+1
            NELE(L) = JRRAY(1,3)
            NOD1(L) = JRRAY(1,5)
            NOD2(L) = JRRAY(1,6)
            NOD3(L) = JRRAY(1,7)
            NOD4(L) = JRRAY(1,8)
            NOD5(L) = JRRAY(1,9)
            NOD6(L) = JRRAY(1,10)
            NOD7(L) = JRRAY(1,11)
            NOD8(L) = JRRAY(1,12)


        ELSE
            T=2
        END IF

500 CONTINUE
600 TOTVOL = 0
        DO 900 I = 1,L
            LEVEL = 0
            DO 800 J = 1,N
                IF(LEVEL.EQ.8) GO TO 850

* IF-THEN LOOP CHECKS AND GETS THE COORDINATES FOR THE 8 NODE POINTS
* FOR EACH ELEMENT, THESE COORDINATES ARE LATER USED TO FIND VOLUME

            IF (NODE(J).EQ.NOD1(I)) THEN
                LEVEL=LEVEL+1
                PA =J
            END IF
            IF (NODE(J).EQ.NOD2(I)) THEN
                LEVEL = LEVEL + 1
                PB =J
            END IF
            IF (NODE(J).EQ.NOD3(I)) THEN
                LEVEL = LEVEL + 1
                PC =J
            END IF
            IF (NODE(J).EQ.NOD4(I)) THEN
                LEVEL = LEVEL + 1
                PD =J
            END IF
            IF (NODE(J).EQ.NOD5(I)) THEN
                LEVEL = LEVEL + 1
                PE =J
            END IF
            IF (NODE(J).EQ.NOD6(I)) THEN
                LEVEL = LEVEL + 1
                PF =J
            END IF
            IF (NODE(J).EQ.NOD7(I)) THEN
                LEVEL = LEVEL + 1
                PG =J
            END IF
            IF (NODE(J).EQ.NOD8(I)) THEN
                LEVEL = LEVEL + 1
                PH =J
            END IF
800     CONTINUE
```

```
*  THE FOLLOWING CALCULATION WILL DETERMINE THE VOL OF EACH ELEMENT

   850      AJ1=-X(PA)-X(PB)+X(PC)+X(PD)-X(PE)-X(PF)+X(PG)+X(PH)
            AJ4=-X(PA)-X(PB)-X(PC)-X(PD)+X(PE)+X(PF)+X(PG)+X(PH)
            AJ7=-X(PA)+X(PB)+X(PC)-X(PD)-X(PE)+X(PF)+X(PG)-X(PH)
            AJ2=-Y(PA)-Y(PB)+Y(PC)+Y(PD)-Y(PE)-Y(PF)+Y(PG)+Y(PH)
            AJ5=-Y(PA)-Y(PB)-Y(PC)-Y(PD)+Y(PE)+Y(PF)+Y(PG)+Y(PH)
            AJ8=-Y(PA)+Y(PB)+Y(PC)-Y(PD)-Y(PE)+Y(PF)+Y(PG)-Y(PH)
            AJ3=-Z(PA)-Z(PB)+Z(PC)+Z(PD)-Z(PE)-Z(PF)+Z(PG)+Z(PH)
            AJ6=-Z(PA)-Z(PB)-Z(PC)-Z(PD)+Z(PE)+Z(PF)+Z(PG)+Z(PH)
            AJ9=-Z(PA)+Z(PB)+Z(PC)-Z(PD)-Z(PE)+Z(PF)+Z(PG)-Z(PH)

            VOLA=AJ1*AJ5*AJ9+AJ2*AJ6*AJ7+AJ3*AJ4*AJ8-AJ3*AJ5*AJ7
            VOLB=-AJ2*AJ4*AJ9-AJ1*AJ6*AJ8
            VOL(I) = 0.0156250*(VOLA+VOLB)
            TOTVOL = TOTVOL + VOL(I)
   900 CONTINUE
       TOTVOL = 4*TOTVOL


*
*  THIS PART OF THE PROGRAM IS USED TO OBTAIN THE AVERAGE FLUX
*     FOR EACH ELEMENT
*
       SUM = 0
       NUMB = 1
       KB = 0
       DO 2000 KA = 1,99999
          IF(NUMB.LE.27) THEN
            READ(32,1500,END=2100) NEL,NPNT,FLUX
   1500     FORMAT(2I5,E10.3)
            SUM = SUM + FLUX
            NUMB = NUMB + 1
          ELSE
            KB = KB + 1

*  THE AVERAGE FLUX IS MULTIPLIED BY 1054.5 TO CONVERT FROM
*                                        BTU/SEC TO WATTS

            AVE(KB) =(SUM/27)*1054.5
            NELA(KB) = NEL
            SUM = 0
            NUMB = 1
          END IF
  2000 CONTINUE

  2100 TOTPOW = 0

*  THIS PORTION OF THE PROGRAM IS USED TO WRITE OUT ALL THE PERTINENT
*    INFORMATION TO FILE FOR054.DAT
*          ALSO THE TOTAL POWER IS SUMMED UP BELOW
*
```

```
      WRITE(54,2150)
2150  FORMAT(1H1,8X,33HTUNNEL-9 GRAPHITE HEATER ELEMENT /)
      WRITE(54,2200)
2200  FORMAT(1X,6X,37HELECTRICAL RESISTANCE HEAT GENERATION////)
      WRITE(54,2250)
2250  FORMAT(1X,7HELEMENT,5X,6HVOLUME,7X,8HAVE FLUX,7X,10HAVE POWER /)
      WRITE(54,2300)
2300  FORMAT(1X,10X,11H(CUBIC IN.),4X,11H(WATT/IN^3),6X,7H(WATTS)/)

      DO 2750 IEL = 1 , L
         POW = VOL(IEL) * AVE(IEL)
         WRITE(54,2500)NELE(IEL),VOL(IEL),AVE(IEL),POW
2500     FORMAT(I7,4X,3(E10.3,5X))
         TOTPOW = TOTPOW + POW
2750  CONTINUE

      TOTPOW = 4*TOTPOW

      WRITE(54,2800)
2800  FORMAT(1X///1X,2X,11HTOTAL POWER,12X,13HTOTAL VOLUME /)
      WRITE(54,2900) TOTPOW,TOTVOL
2900  FORMAT(E10.3,1X,5HWATTS,7X,E10.3,1X,9HCUBIC IN.)
3000  END FILE 54
        STOP
        END
```

APPENDIX B

ABAQUS INPUT FILES

```
ABAQUS THERMAL/ELECTRIC ANALOGUE INPUT FILE
REV-J HEATER
653 KWATTS

*BOUNDARY
INBASE,11,,57.748
LIGA,11,,0.0
*MATERIAL
*CONDUCTIVITY, TYPE=ISO
** UNITS ARE (OHM-IN)**-1
2032.0
*RESTART,WRITE
*STEP, LINEAR
*HEAT TRANSFER, STEADY STATE
*NODE PRINT
2,,,,2,2,,2
*EL FILE, TEMPS, HEAT FLUX, COORDS,LOADS
*NODE FILE
2,,,,2,2,,2
*END STEP
```

```
ABAQUS THERMAL ANALYSIS INPUT FILE
REV-J GRAPHITE HEATER
END HEAT

*MATERIAL
*CONDUCTIVITY, TYPE=ISO
** UNITS=BTU/IN-SEC-F
9.745E-4, 70.0
7.731E-4, 500.0
5.763E-4, 1000.0
4.537E-4, 1500.0
3.773E-4, 2000.0
3.356E-4, 2500.0
3.055E-4, 3000.0
2.870E-4, 3500.0
2.685E-4, 4000.0
2.523E-4, 4500.0
2.291E-4, 5000.0
*RESTART,WRITE
*STEP, CYCLE=100
*HEAT TRANSFER, STEADY STATE, TEMTOL=10
*RADIATE, ZERO=-460.0
** EMISSIVITY=.85, STEFAN-BOLTZMAN =
** 3.303E-15 BTU/SQ.IN.-SEC-F**4
CUTOUT,R5,3100.0,2.807E-15
CROWN,R4,3100.0,2.807E-15
ODDOUT,R6,3100.0,2.807E-15
*FILM
** UNITS = BTU/SEC-SQ.IN.-F
CUTOUT,F5, 3100.0, 2.272E-04
CROWN,F4, 3100.0, 2.272E-04
ODDOUT,F6, 3100.0, 2.272E-04
EVENIN,F4, 3100.0, 2.272E-04
*DFLUX
ALL,BFNU
*EL PRINT, TEMPS, HEAT FLUX, COORDS,LOADS
*NODE PRINT
2,,,,,2,2,,2
*EL FILE, TEMPS, HEAT FLUX, COORDS,LOADS
*NODE FILE
2,,,,,2,2,,2
*END STEP
```

```
ABAQUS STRESS ANALYSIS INPUT FILE
CLAMPED BASE
REV-J GRAPHITE HEATER

*MATERIAL
*ELASTIC, TYPE=ISOTROPIC
1.31E+06, 0.13, 70.0
1.34E+06, 0.13, 932.0
1.50E+06, 0.13, 1832.0
1.65E+06, 0.13, 2732.0
1.73E+06, 0.13, 3632.0
1.69E+06, 0.13, 4532.0
1.62E+06, 0.13, 5432.0
*EXPANSION, ZERO=70.0, TYPE=ISO
** MEAN COEFF'S OF EXPANSION. REF STRESS-FREE TEMP=70.0 F
1.75E-06, 70.0
3.33E-06, 2500.0
3.60E-06, 5000.0
*BOUNDARY
XZERO,2,,0.0
LIGA,2,,0.0
INBASE,1,,0.0
INBASE,3,,0.0
OUTBAS,1,,0.0
OUTBAS,3,,0.0
*RESTART,WRITE
*STEP, LINEAR
*STATIC
*TEMPERATURE, FILE=15, BSTEP=1(INC=1),ESTEP=1(INC=1)
*NODE PRINT
2,,,,1,1
*EL FILE, TEMPS, COORDS
2,2
2
2,2,1,2
*NODE FILE
2,,,,,2,2
*END STEP
```

APPENDIX C

FREE CONVECTION HEAT TRANSFER FILM COEFFICIENT
CALCULATION FOR MACH-14 END HEAT CONDITIONS

Heater Gas Conditions: Gas = Nitrogen
Pressure = 22,000 psi= 1496 atm
Temp. = 3100°F (=3560°R = 1977°K)

First compute Grashof Number to determine whether laminar or turbulent conditions apply:

$$Gr = g(T_s - T_g)\beta L^3 (\rho/u)^2$$

where:

T_s= Heater Surface Temperature= 5000°F (=5460°R =3033°K)
T_g= Nitrogen Gas Temperature
β = Coefficient of Expansion = $1/T_g$ = 1/3560°R
g = gravity constant = 32 ft/sec/sec
L = vertical distance from Heater Element Base
ρ = Nitrogen Density @ T_{ave}
u = Viscosity of Nitrogen @ T_{ave}
T_{ave} = Average Film Temperature = $(T_g + T_s)/2$= 2505°K = 4510°R

Compute density and viscosity of nitrogen gas:

$$\rho \bigg|_{T_{ave}} = 11 \text{ lb/cu ft (at 22,000 psi from nitrogen table)}$$

$$u \bigg|_{T_{ave}} = 6.111 \times 10^{-5} \text{ lbm/sec-ft}$$

Compute Grashof Number:

$$G_r = (32 \text{ ft/sec2}) \left(\frac{5460-3560}{3560°R}\right)(4 \text{ ft})^3 \left(\frac{11 \text{ lb/cu ft}}{(6.111 \times 10^{-5} \text{ lbm/sec-ft})}\right)^2$$

Gr= 3.686 E13

The following criteria apply:

Laminar Convection: Gr < 1.0 E+09
Turbulent Convection: Gr ≥ 1.0 E+09

It turns out that the flow is laminar for only an inch or so from the heater element base, so turbulent flow is assumed to exist over the full length of the heater. The average film coefficient, h, can be gotten then from Figure 7-4, Reference C-1, for vertical cylinders.

$$\bar{h} = .021 \ (k/L)(Gr*Pr)^{0.4}$$

Where:

$\bar{h}$ = Average Film Coefficient
k = Thermal Conductivity of gas at T_{ave}
L = Vertical height of Heater = 4 ft
Gr = Grashof Number
Pr = Prandtl Number = c_p*u/k
c_p = Specific Heat of gas at T_{ave}

Compute conductivity and specific heat at average film temperature:

$$k \quad (@4510 \ R) = 0.0975 \ BTU/hr\text{-}ft\text{-}R$$

$$c_p \quad " \quad = 0.305 \ BTU/lbm \ R$$

Then

$$Pr = (.305)(.22)/(0.0975) = 0.689$$

Evaluate Film Coefficient:

$$\bar{h} = (.021) \ (0.0975) \ (.689 * 3.686 \ E13)^{0.4} \ /4$$

$$\bar{h} = \underline{117.3 \ BTU/hr\text{-}sq \ ft\text{-}R}$$

REFERENCES

C-1. Kreith, F., _Principles of Heat Transfer_, International Textbook Co., New York, NY, 1973.

APPENDIX D

TENSILE STENGTH AND STRAIN-TO-FAILURE
EXPERIMENTAL DATA FOR HEATER GRAPHITE

The Strength Data presented here was obtained from Reference D-1 and D-2. The data are for 2020-type graphite manufactured by the Stackpole Corporation and YU60ST graphite made by Ultracarbon Corporation.

APPENDIX D. STRAIN TO FAILURE AT 2000°F

LEGEND

□ = AXIAL

O = HOOP

AXIAL

60 DATA POINTS

AVERAGE = 0.35237E − 02
VARIANCE = 0.19866E − 06
STD. DEV = 0.44572E − 03
COV = 0.12649E + 00

HOOP

14 DATA POINTS

AVERAGE = 0.34929E − 02
VARIANCE = 0.19764E − 06
STD. DEV = 0.44456E − 03
COV = 0.12728E + 00

PROBABILITY OF FAILURE (PERCENT)

STRAIN (IN/IN)

×10⁻³
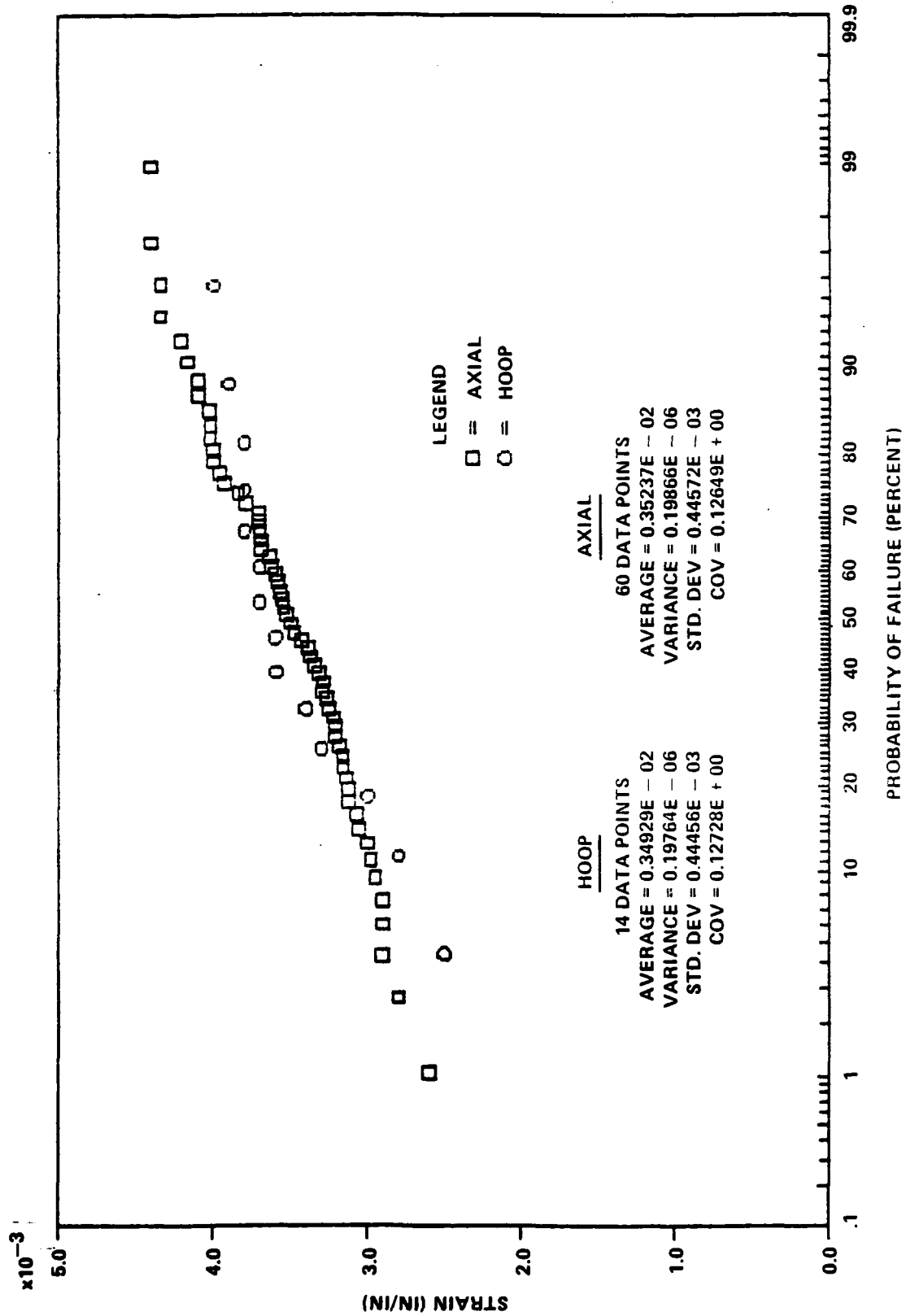
APPENDIX D. TENSILE STRENGTH AT 2000°F

LEGEND

□ = AXIAL
○ = HOOP

AXIAL
60 DATA POINTS
AVERAGE = 0.41315E + 01
VARIANCE = 0.12248E + 00
STD. DEV = 0.34997E + 00
COV = 0.84708E − 01

HOOP
14 DATA POINTS
AVERAGE = 0.44086E + 01
VARIANCE = 0.43587E + 00
STD. DEV = 0.66021E + 00
COV = 0.14976E + 00

PROBABILITY OF FAILURE (PERCENT)

STRESS (KSI)
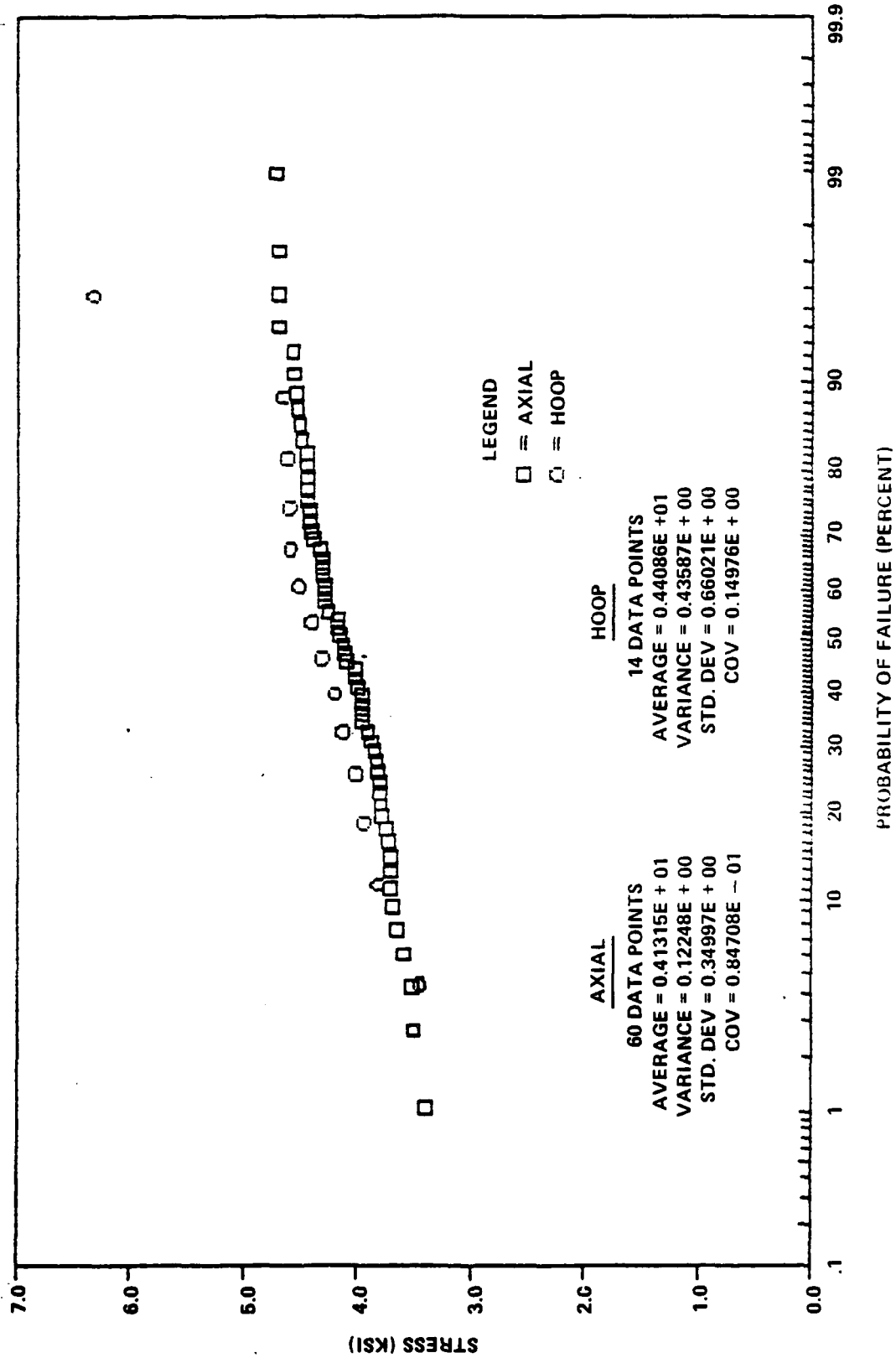
REFERENCES

D-1. Southern Research Institute, <u>Evaluation and Comparison of Graphite Heater Tube Materials Used in the Hypervelocity Wind Tunnel</u>, SoRI-EAS-86-508-5787-I-F, Southern Research Institute, Birmingham, AL, Jul 1986.

D-2. Southern Research Institute, <u>Test and Evaluation of Carbon-Carbon Nosetip Materials: Evaluation of Failed Heater Elements</u>, SoRI-Eas-82-770-4179-8-I-F, Southern Research Institute, Birmingham, AL, Nov 1982.

DISTRIBUTION

	Copies		Copies
Center for Naval Analyses		Internal Distribution:	
4401 Fort Avenue		K	1
P.O. Box 16268		K20	1
Alexandria, VA 22302-0268	1	K22	1
		K22 (E. Becker)	1
Calspan Corporation		K22 (W. Dorsey)	1
AEDC Division		K22 (R. Edwards)	1
Attn: R.K. Matthews	1	K22 (M. Fung)	1
Aerophysics Branch		K22 (D. Vavrick)	1
Von Karman Facility		K22 (L. Zentz)	1
Arnold Air Force Station,		K23	1
TN 37389		K23 (J. Etheridge)	1
		K23 (C. Higgins)	1
Materials Sciences Corporation		K23 (E. Larach)	1
Attn: Kent Buesking	1	K23 (M. Metzger)	10
Gwynedd Plaza II		K23 (D. Newell)	1
Bethlehem Pike		K23 (C. Rozanski)	1
Spring House, PA 19477		K23 (J. Waldo)	1
		K23 (R. Waser)	1
Southern Research Institute		K24	1
Attn: Sam Causey	1	K24 (R. Driftmyer)	1
2000 Ninth Ave South		R14 (R. Kavetsky)	1
P.O. Box 55305		E231	2
Birmingham, AL 35255-5305		E232	15

Library of Congress
Attn: Gift and Exchange
       Division   4
Washington, DC 20540

Defense Technical Information
  Center
Cameron Station
Alexandria,VA 22304-6145   12